From the Department of Laboratory Medicine, Division of Pathology
Karolinska Institutet, Stockholm, Sweden

PANCREATIC CANCER: INVESTIGATION OF THE PROGNOSTIC SIGNIFICANCE OF TUMOR IMMUNOPHENOTYPE AND ESTABLISHMENT OF A NOVEL EX-VIVO TISSUE SLICE CULTURE SYSTEM FOR DRUG SENSITIVITY TESTING

Carlos Fernández Moro

Karolinska Institutet

Stockholm 2021

Published by Karolinska Institutet.
Printed by Universitetsservice US-AB, 2021

ISBN 978-91-8016-269-2
Cover illustration by Carlos Fernández Moro. Left: Precision-cut tissue slice of human PDAC cultured for 72 h and immunostained with CD15 (brown) and CK19 (red). Right: Detail in H&E staining of a cultured PDAC tissue slice showing an outgrowth of severely damaged cancer cells after selenium treatment.

Pancreatic cancer: investigation of the prognostic significance of tumor immunophenotype and establishment of a novel ex-vivo tissue slice culture system for drug sensitivity testing

THESIS FOR DOCTORAL DEGREE (Ph.D.)

By

Carlos Fernández Moro

The thesis will be defended in public at 4X, Alfred Nobels Allé 8 Campus Flemingsberg, 17th June 2021, 10.00 AM.

Principal Supervisor:
Professor Caroline Sophie Verbeke
University of Oslo
Institute of Clinical Medicine
Department of Pathology

Co-supervisors:
Professor Mikael Björnstedt
Karolinska Institute
Department of Laboratory Medicine
Division of Pathology

Professor Matthias Löhr
Karolinska Institute
Department of Clinical Science,
Intervention and Technology

Opponent:
Professor Karin Jirström
Lund University
Department of Clinical Sciences
Division of Therapeutic Pathology

Examination Board:
Professor Charlotte Rolny
Karolinska Institute
Department of Oncology-Pathology

Professor Roger Henriksson
Umeå University
Department of Radiation Sciences
Division of Oncology

Professor Göran Andersson
Karolinska Institute
Department of Laboratory Medicine
Division of Pathology

What Cancer Cannot Do

Cancer is so limited...

It cannot cripple love

It cannot shatter hope

It cannot corrode faith

It cannot destroy peace

It cannot kill friendship

It cannot suppress memories

It cannot silence courage

It cannot invade the soul

It cannot steal eternal life

It cannot conquer the spirit

- Author Unknown

Dedicated to bringing hope to all patients suffering from cancer and to their families.

"Love is the bridge between you and everything."

- Rumi

POPULAR SCIENCE SUMMARY OF THE THESIS

Pancreatic cancer is a disease in which malignant (cancer) cells develop and grow unrestrained by usual control mechanisms in the pancreas, an organ located in the abdomen behind the lower part of the stomach. As the tumor grows, cancer cells invade neighboring tissues and organs, such as the distal bile duct, a tubular structure that crosses the pancreas to allow a fluid called bile to drain from the liver into the small intestine. In addition, pancreatic cancer cells tend to grow into vessels and nerves and travel along them to other tissues and organs, even distant ones, like the liver or the lungs. Once pancreatic cancer cells reach these distant organs, they form new cancer growths, called metastases, that progressively occupy and destroy these organs, causing considerable, and ultimately fatal, worsening of patient's condition.

Once pancreatic cancer is detected, there are various possible treatments, but unfortunately, to date they are not effective enough to eliminate all cancer cells and cure the patient. The most effective treatment is to remove the tumor by surgical operation, following which - after a few weeks of recovery – the patient is treated with anti-cancer drugs (so-called chemotherapy). Chemotherapy kills and damages a part of the cancer cells and slows down the disease, but after months of treatment, the cancer cells change to become unaffected by the chemotherapy and resume their uncontrolled growth.

There is an urgent need to develop new, more effective treatments for pancreatic cancer, like what has been achieved for other cancer types, such as breast and bowel cancer. These were also often fatal some years ago, but now there are treatments that are very effective to slow down and even cure the disease.

The work in this thesis aims at contributing to the current efforts in the medical and scientific community to develop better treatment for patients with pancreatic cancer. This endeavor was undertaken in three ways:

First, by showing that not all pancreatic cancers are identical when it comes to their microscopic appearance and aggressiveness, by investigating whether this could be the basis for distinguishing between different subtypes. For example, in some pancreatic cancers the tumor cells resemble those from bowel cancer, they usually grow more slowly, and patient survival is longer. Discrimination between distinct cancer subtypes can be done more precisely by using a special technique that stains the cells depending on the presence of some special components, called proteins, that appear in certain but not in other cancer subtypes.

Second, by establishing a new method that allows to test in the laboratory which anti-cancer drugs may be more effective to kill an individual patient's cancer cells. This is currently done by testing different drugs on either commercially available isolated cancer cells or animals (usually mice) with pancreatic cancer. But even if results are promising in these experiments, the same drugs often have a disappointing effect when given to humans, likely because both the cancer cells and the surrounding tissues are very different in patients than they are in the experiments. With the new technique, a small piece (up to 1 cm in size) of tissue is taken from the patient's pancreatic cancer which has been removed by the surgeon, and this tissue is cut into very thin slices (one third of mm thick). We could show that these pancreatic

cancer slices can be maintained intact and alive in the laboratory for at least 4 days. This gives us the possibility to search (in the laboratory) for effective anti-cancer drugs by testing them in the tumor slices, in which the cancer cells and surrounding tissues are very similar to those in the patient. Therefore, drugs that show good effect when using this new method, are likely to be also effective when tested in patients.

Third, we tested the efficacy of selenium, a nutrient that is essential for human health, as an anti-cancer drug in the thin slices of pancreatic cancer as described above. Remarkably, most pancreatic cancer cells were killed after treating them with selenium, while the neighboring (normal) cells remained alive. That is, selenium was effective specifically against pancreatic cancer and this effect occurred at doses that can safely be administered to patients without causing serious toxic side effects.

In summary, the work laid down in this thesis, that is the distinction between pancreatic cancer subtypes of different aggressiveness, the new laboratory model based on tumor slices to test for effective drugs, and the demonstration of promising anti-cancer effects of selenium, will contribute to the development of more effective treatment that is better suited for the individual pancreatic cancer patient.

ABSTRACT

Pancreatic ductal adenocarcinoma (PDAC), commonly referred to as pancreatic cancer, is associated with a dismal 5-year overall survival of 9 to 6 %. A major reason for the high mortality is the pronounced resistance to treatment. There is urgent need for the development of novel, effective therapies and for a better understanding as to why some tumors respond better to treatment than others.

The process for conventional drug testing relies significantly on cell lines and genetically engineered mouse models. Even if these models recapitulate some of the features of human pancreatic cancer, there are significant limitations, mainly the lack of the native tumor microenvironment and the use of a host that belongs to another species and may be immunocompromised.

In **Paper I,** a large cohort (n = 409) of adenocarcinomas from the main anatomical locations in the pancreatobiliary system is analyzed by immunohistochemistry with a panel of up to 27 antibodies. Hierarchical clustering and differential expression analysis reveal three immunohistochemical tumor types (extrahepatic pancreatobiliary, intestinal and intrahepatic cholangiocarcinoma) and their distinguishing markers. Among patients who underwent surgical resection of the primary tumor, the intestinal type showed an adjusted hazard ratio of 0.19 for overall survival (p value = 0.014) as compared to the extrahepatic pancreatobiliary type. Furthermore, the characteristic immunohistochemical profile supports the positive diagnosis of intrahepatic cholangiocarcinoma, which is commonly regarded as a diagnosis of exclusion. The presented integrative immunohistochemical classification may contribute to improve diagnosis and prognostic stratification for patients with adenocarcinomas of the pancreatobiliary system.

Paper II introduces a novel ex-vivo model of precision-cut tissue slices that allows culturing of human PDAC including the native tumor microenvironment. Fresh tumor tissue samples (n = 12) were obtained from surgical resection specimens, cut into 350 µm thick tissue slices, and cultured for at least 96 h. Every 24 h, tissue slices were harvested and processed for analysis, including histomorphology, transmission electron microscopy and immunohistochemistry. These revealed good morphological preservation and ultrastructural integrity of the tissue slices, including cancerous, stromal, and immune cell populations. Each tumor retained its characteristic histological and cytological features and grade of differentiation throughout the entire culture period. A cancerous and, to a lesser extent, non-neoplastic cell outgrowth covered gradually the surface of the tissue slices, while tumor cells retained their proliferative (Ki67) and metabolic (pS6 mTOR pathway) activity. This culture system is a close surrogate of the parent tumor and harbors promising potential for drug sensitivity testing and personalized treatment of PDAC.

Paper III is a continuation study in which five tissue slice cultures of human PDAC (from Paper II) are analyzed at the whole transcriptome level (RNASeq). Findings at 24 h intervals (24-72 h of culture) are compared to baseline (0 h, non-cultured tissue). On differential expression analysis, only a limited number of genes (median range 10-25) were up- or downregulated during culture. One culture with morphologically visible regions of necrosis/apoptosis (0-18 % total slice area) showed upregulation of VEGFA and PTGS2.

Pathway analysis suggested for this culture a highly significant probability of activation of apoptosis via HIF-1/quercetin/NF-κB/AP-1 interaction pathways. These results support that the transcriptome of the parent tumor is largely preserved in ex-vivo cultured tissue slices of PDAC, and that transcriptomic analysis is a valuable complement to morphology for evaluation of the tissue slices.

Finally, in **Paper IV**, the previously established (in Papers II and III) ex-vivo model of precision-cut tissue slices is used for drug sensitivity testing in nine samples of surgically resected human PDAC. PDAC tissue slices were exposed to selenium compounds (selenite and methylselenocysteine) at various concentrations and gemcitabine 1 μM during 48 h of culture. Selenium compounds administered at concentrations below the maximum tolerated dose in humans significantly reduced PDAC cell viability ($p < 0.02$) and decreased outgrowth of viable tumor cells onto the tissue surface ($p < 0.05$), while non-neoplastic tissues remained preserved. Transcriptomic analysis revealed downregulation of CEMIP, PLOD2, DDR2 and P4HA1, genes that are involved in extracellular matrix modulation, cancer growth and metastatic potential, while the cell death-inducing genes ATF3 and ACHE were significantly upregulated ($p < 0.0001$).

In conclusion, the results of this thesis support the value of immunohistochemical profiling for the diagnosis of prognostically significant subtypes of periampullary adenocarcinomas. The findings confirm the relevance of the precision-cut tissue slice culture model for anticancer drug sensitivity testing and the potential of selenium compounds as candidate drugs for the treatment of PDAC.

LIST OF SCIENTIFIC PAPERS

This thesis is based on the following peer-reviewed publications and manuscript.

I. **Carlos Fernández Moro**, Alejandro Fernandez-Woodbridge, Melroy Alistair D'souza, Qianni Zhan, Béla Bozoky, Senthil Vasan Kandaswamy, Piera Catalano, Rainer Heuchel, Sonia Shtembari, Marco Del Chiaro, Olof Danielsson, Mikael Björnstedt, Johannes-Matthias Löhr, Bengt Isaksson, Caroline Sophie Verbeke, Béla Bozóky.
Immunohistochemical Typing of Adenocarcinomas of the Pancreatobiliary System Improves Diagnosis and Prognostic Stratification. *PLoS One. 2016 Nov 9;11(11):e0166067. doi: 10.1371/journal.pone.0166067.*

II. Sougat Misra* & **Carlos Fernández Moro***, Marco Del Chiaro, Soledad Pouso Elduayen, Anna Sebestyén, Johannes-Matthias Löhr, Mikael Björnstedt & Caroline Sophie Verbeke.
Ex Vivo Organotypic Culture System of Precision-Cut Slices of Human Pancreatic Ductal Adenocarcinoma. *Scientific Reports. 2019 Feb 14;9(1):2133. doi: 10.1038/s41598-019-38603-w*.

III. Mehran Ghaderi* & **Carlos Fernández Moro***, Soledad Pouso Elduayen, Emilie Hultin, Caroline Sophie Verbeke, Mikael Björnstedt & Joakim Dillner.
Genome-wide Transcriptome Profiling of Ex-Vivo Precision-Cut Slices from Human Pancreatic Ductal Adenocarcinoma. *Scientific Reports. 2020 Jun 3;10(1):9070. doi: 10.1038/s41598-020-65911-3*.

IV. **Carlos Fernández Moro*** & Arun Kumar Selvam* & Mehran Ghaderi*, Marco Gerling, Béla Bozóky, Soledad Pouso Elduayen, Joakim Dillner & Mikael Björnstedt.
Selenium Compounds Exert Tumor-specific Cytotoxicity on Pancreatic Cancer and Suppress DDR2 and CEMIP in Human Organotypic Cultures. *Manuscript*.

* Authors contributed equally.

RELATED RESEARCH ARTICLES CO-AUTHORED BY THE DEFENDANT NOT INCLUDED IN THE THESIS

• Benedek Bozóky, **Carlos Fernández Moro**, Carina Strell, Ingemar Ernberg, Laszlo Szekely, Marco Gerling, Béla Bozóky. Basal-to-classical phenotypic switch of pancreatic cancer cells upon integration into the duodenal epithelium. Preprint bioRxiv 2021.02.01.429212; doi: https://doi.org/10.1101/2021.02.01.429212.

• Laia Gorchs, Sultan Ahmed, Chanté Mayer, Alisa Knauf, **Carlos Fernández Moro**, Mattias Svensson, Rainer Heuchel, Elena Rangelova, Peter Bergman, Helen Kaipe. The vitamin D analogue calcipotriol promotes an anti-tumorigenic phenotype of human pancreatic CAFs but reduces T cell mediated immunity. Sci Rep. 2020 Oct 15;10(1):17444. doi: 10.1038/s41598-020-74368-3.

• Hassan Alkharaan, Liyan Lu, Giorgio Gabarrini, Asif Halimi, Zeeshan Ateeb, Michał J Sobkowiak, Haleh Davanian, **Carlos Fernández Moro**, Leif Jansson, Marco Del Chiaro, Volkan Özenci, Margaret Sällberg Chen. Circulating and Salivary Antibodies to Fusobacterium nucleatum Are Associated With Cystic Pancreatic Neoplasm Malignancy. Front Immunol. 2020 Aug 28;11:2003. doi: 10.3389/fimmu.2020.02003.

• K J Norberg, X Liu, **C Fernández Moro**, C Strell, S Nania, M Blümel, A Balboni, B Bozóky, R L Heuchel, J M Löhr. A Novel Pancreatic Tumour and Stellate Cell 3D Co-Culture Spheroid Model. BMC Cancer. 2020. 20(1):475.

• Thomas Held, Caroline S. Verbeke, Oliver Strobel, Wiktor Rutkowski, Christina Villard, **Carlos Fernández Moro**, Marco Del Chiaro, Markus Büchler, Rainer Heuchel, Matthias Löhr. Immunohistochemical profiling of liver metastases and matched-pair analysis in patients with metastatic pancreatic ductal adenocarcinoma. Pancreatology. 2019 Oct;19(7):963-970. https://doi.org/10.1016/j.pan.2019.09.005.

• Gaiser RA, Pessia A, Ateeb Z, Davanian H, **Fernández Moro C**, Alkharaan H, Healy K, Ghazi S, Arnelo U, Valente R, Velagapudi V, Sällberg Chen M, Del Chiaro M. Integrated targeted metabolomic and lipidomic analysis: A novel approach to classifying early cystic precursors to invasive pancreatic cancer. Sci Rep. 2019 Jul 15;9(1):10208. doi: 10.1038/s41598-019-46634-6.

• Gorchs L, **Fernández Moro C**, Bankhead P, Kern KP, Sadeak I, Meng Q, Rangelova E, Kaipe H. Human Pancreatic Carcinoma-Associated Fibroblasts Promote Expression of Co-inhibitory Markers on CD4+ and CD8+ T-Cells. Front Immunol. 2019 Apr 24;10:847.

• Gaiser RA, Halimi A, Alkharaan H, Lu L, Davanian H, Healy K, Hugerth LW, Ateeb Z, Valente R, **Fernández Moro C**, Del Chiaro M, Sällberg Chen M. Enrichment of oral microbiota in early cystic precursors to invasive pancreatic cancer. Gut. 2019 Mar 14. pii: gutjnl-2018-317458.

• Ateeb Z, Valente R, Pozzi-Mucelli RM, Malgerud L, Schlieper Y, Rangelova E, **Fernandez-Moro C**, Löhr JM, Arnelo U, Del Chiaro M. Main pancreatic duct dilation greater than 6 mm is associated with an increased risk of high-grade dysplasia and cancer in IPMN patients. Langenbecks Arch Surg. 2019 Feb;404(1):31-37.

•Meng Q, Valentini D, Rao M, **Moro CF**, Paraschoudi G, Jäger E, Dodoo E, Rangelova E, Del Chiaro M, Maeurer M. Neoepitope targets of tumour-infiltrating lymphocytes from patients with pancreatic cancer. Br J Cancer. 2019 Jan;120(1):97-108. doi: 10.1038/s41416-018-0262-z.

• **Moro CF**, Bozóky B, Gerling M. Growth patterns of colorectal cancer liver metastases and their impact on prognosis: a systematic review. BMJ Open Gastroenterol. 2018 Jul 27;5(1):e000217. doi: 10.1136/bmjgast-2018-000217.

• Malgerud L, Lindberg J, Wirta V, Gustafsson-Liljefors M, Karimi M, **Moro CF**, Stecker K, Picker A, Huelsewig C, Stein M, Bohnert R, Chiaro MD, Haas SL, Heuchel RL, Permert J, Maeurer MJ, Brock S, Verbeke CS, Engstrand L, Jackson DB, Grönberg H, Matthias Löhr J. Bioinformatory-assisted analysis of next-generation sequencing data for precision medicine in pancreatic cancer. Mol Oncol. 2017;11:1413-1429.

• Strell C, Norberg KJ, Mezheyeuski A, Schnittert J, Kuninty PR, **Moro CF**, Paulsson J, Schultz NA, Calatayud D, Löhr JM, Frings O, Verbeke CS, Heuchel RL, Prakash J, Johansen JS, Östman A. Stroma-regulated HMGA2 is an independent prognostic marker in PDAC and AAC. Br J Cancer. 2017;117:65-77.

• Li X, Nania S, Fejzibegovic N, **Moro CF**, Klopp-Schulze L, Verbeke C, Löhr JM, Heuchel RL. Cerulein-induced pancreatic fibrosis is modulated by Smad7, the major negative regulator of transforming growth factor-β signaling. Biochim Biophys Acta. 2016 Sep;1862(9):1839-46.

• Kamposioras K, Anthoney A, **Fernández Moro C**, Cairns A, Smith AM, Liaskos C, Verbeke CS. Impact of intrapancreatic or extrapancreatic bile duct involvement on survival following pancreatoduodenectomy for common bile duct cancer. Br J Surg. 2014 Jan;101(2):89-99. doi: 10.1002/bjs.9367.

CONTENTS

LIST OF ABBREVIATIONS

5-FU	Fluorouracil
ACHE	Acetylcholinesterase
ALK	Anaplastic lymphoma kinase
AP-1	Activator protein 1
ARE	Antioxidant response element
ATF3	Cyclic AMP-dependent transcription factor ATF-3
ATP	Adenosine triphosphate
Bbk	Biobank
BRCA	Breast cancer susceptibility protein
CA	Cancer antigen
CAF	Cancer associated fibroblast
CAR	Chimeric antigen receptor
CCL	Chemokine (C-C motif) ligand
CD	Cluster of differentiation
cDNA	Complementary deoxyribonucleic acid
CDKN2A	Cyclin-dependent kinase inhibitor 2A
CEA	Carcinoembryonic antigen
CEACAM	Carcinoembryonic antigen-related adhesion molecules
CEMIP	Cell migration-inducing and hyaluronan-binding protein
CDX2	Caudal-Type Homeobox Protein 2
CI	Confidence interval
CFSE	Carboxyfluorescein succinimidyl ester
CK	Cytokeratin
CMRL	Connaught Medical Research Laboratories
CONKO	Charité Onkologie
Cox2	Cyclooxygenase-2
CRYAB	Alpha-crystallin B chain
CTLA-4	Cytotoxic T-lymphocyte-associated protein 4
CTSL	Cathepsin L
CXCL	Chemokine (C-X-C motif) ligand

CXCR	Chemokine (C-X-C motif) receptor
D2-40	Podoplanin
DDR2	Discoidin domain-containing receptor 2
DNA	Deoxyribonucleic acid
DT	Drug testing organotypic slice culture
EBV	Epstein–Barr virus
ECOG	Eastern Cooperative Oncology Group
ECM	Extracellular matrix
EdU	5-ethynyl-2′-deoxyuridine
EMA	Epithelial membrane antigen
EMT	Epithelial-to-mesenchymal transition
EPCAM	Epithelial cell adhesion molecule
ESPAC	European Study Group for Pancreatic Cancer
EU	European Union
FAMMM	Familial atypical multiple mole melanoma
FAP	Fibroblast activation protein
FGF	Fibroblast growth factor
FOLFIRINOX	Folinic acid, fluorouracil, irinotecan and oxaliplatin
FPKM	Fragment per kilobase million
GDPR	General Data Protection Regulation
GemCap	Gemcitabine and capecitabine
GM-CSF	Granulocyte-macrophage colony-stimulating factor
GNAS	Guanine nucleotide-binding proteins (G proteins)
GRCh	Genome Reference Consortium human build
GSH	Glutathione
H2AX	H2A histone family member X
HAS	Hyaluronan synthase
HDAC	Histone deacetylase
H&E	Hematoxylin and eosin
HEPES	4-(2-hydroxyethyl)-1-piperazineethanesulfonic acid
HH	Hedgehog

HIF-1	Hypoxia-inducible factor 1-alpha
HNF	Hepatocyte nuclear factor
HNPCC	Hereditary nonpolyposis colorectal cancer
HR	Hazard ratio
HSF	Heat shock factor
HSB	Heat shock protein family B
IFN	Interferon
IGFBP	Insulin-like growth factor-binding protein
IL	Interleukin
IPA	Indole-3-pyruvic acid
IPMN	Intraductal papillary mucinous neoplasia
JAK	Janus kinase
KRAS	GTPase KRas
KRT	Keratin
KYAT1	Kynurenine aminotransferase 1
LIF	Leukemia inhibitory factor
MAPK	Mitogen-activated protein kinase
MICA	MHC class I chain A
MDSC	Myeloid derived suppressor cell
MEK	Mitogen-activated protein kinase kinase
MHC	Major histocompatibility complex
MLH1	DNA mismatch repair protein Mlh1
μM	Micromolar
MMP	Matrix metalloproteinase
MMR	Mismatch repair
MUC	Mucin
MultTest	Multiple testing
MRP	Multiresistance protein
MSC	Methylselenocysteine
MSH2	DNA mismatch repair protein Msh2
MT-ND	Mitochondrially encoded NADH:ubiquinone oxidoreductase

	core subunit
MT-CO	Mitochondrially encoded cytochrome C oxidase
MT-CYB	Mitochondrially encoded cytochrome B
mTOR	Mammalian target of rapamycin
NADH	Nicotinamide adenine dinucleotide + hydrogen
NCT	National clinical trial
NF-κB	Nuclear factor kappa-light-chain-enhancer of activated B cells
NK	Natural killer
NKG	Natural killer group
OS	Overall survival
OT	Organotypic slice culture
P4HA1	Prolyl 4-hydroxylase subunit alpha-1
PALB2	Partner and localizer of BRCA2
PanIN	Pancreatic intraepithelial neoplasia
PARP	Poly (ADP-ribose) polymerase
PDAC	Pancreatic ductal adenocarcinoma
PDGF	Platelet-derived growth factor
PD-1	Programmed cell death protein 1
PD-L1	Programmed cell death-ligand 1
PenStrep	Penicillin-streptomycin
PI	Propidium iodide
PLOD2	Procollagen-lysine,2-oxoglutarate 5-dioxygenase 2
PMAIP1	Phorbol-12-myristate-13-acetate-induced protein 1
pN	Pathological lymph node status
PRO	Proliferative
PRSS1	Serine Protease 1, Trypsin-1
pS6	Phosphorylated S6
pT	Pathological tumor stage
PTGS	Prostaglandin-endoperoxide synthase
PSC	Pancreatic stellate cell

RankProd	Rank Product
RNA	Ribonucleic acid
ROC	Receiver operating characteristic curve
ROS	Reactive oxygen species
ROS1	Proto-oncogene tyrosine-protein kinase ROS
SAM	Significance analysis of microarrays
Se	Sodium selenite
Shh	Sonic hedgehog
SMA	Smooth muscle actin
SMAD	Mothers against decapentaplegic homolog
SR-FLICA	Sulforhodamine fluorochrome-labeled inhibitor of caspase
STAT	Signal transducer and activator of transcription protein
STK	Serine/threonine-protein kinase
TAM	Tumor associated macrophage
TGF-β	Transforming growth factor beta
Th	T helper
TIL	Tumor infiltrating lymphocyte
TIM-3	T cell immunoglobulin and mucin domain-containing protein 3
TME	Tumor microenvironment
TNF	Tumor necrosis factor
TP53	Tumor Protein P53
TRK	Tropomyosin receptor kinase
TSLP	Thymic stromal lymphopoietin
TUNEL	Terminal deoxynucleotidyl transferase dUTP nick end labeling
VEGFA	Vascular endothelial factor A
WHO	World Health Organization
WST	Water-soluble tetrazolium salt

1 INTRODUCTION

1.1 THE PANCREAS

The pancreas is an elongated organ located retroperitoneally to the left in the posterior abdominal cavity. It can be anatomically divided into head, corpus, and tail. The pancreatic head lies adjacent to the duodenum and is traversed by the ductus choledochus and the pancreatic duct, both of which converge in a common structure, the ampulla of Vater, whose covering with duodenal mucosa is called the major duodenal papilla. This anatomical configuration has important implications for surgical resection of periampullary tumors, this being a standard pancreatoduodenectomy, also called Whipple's procedure.

A major part of the pancreatic parenchyma is composed of acinar cells that are arranged in acini. These produce the digestive enzymes such as lipase, amylase, trypsin, and elastase that are secreted into the small intestine and digest the food stuff, breaking down fats, carbohydrates, and proteins. The enzymes are secreted in an inactive form and conducted from the acini to the ampulla of Vater through the pancreatic ductal system, that is, in a highly isolated and compartmented way to prevent leakage and enzymatic activation in the parenchyma, which may cause pancreatitis (typically acute), with organ damage and inflammation. Together, the acinar tissue and the ductal system form the exocrine component of the pancreas. The endocrine component, which represents around 1-2 % of the parenchyma, is dominated by the islets of Langerhans that receive 10–15 % of the blood flow (1) and secrete directly into it hormones such as insulin and glucagon, which are important for glucose metabolism.

1.2 PANCREATIC CANCER

1.2.1 Epidemiology

Pancreatic cancer is a pressing health problem, with 459,000 new cases worldwide in 2018 (2), and around 1,200 in Sweden in 2016 (3). Worldwide, it is the 12th most common cancer. Pancreatic cancer is currently the fourth leading cause of cancer-related death in the West and predicted to rank second by 2030 (4). Pancreatic ductal adenocarcinoma (PDAC), which originates from the exocrine component, is the most common and lethal form of pancreatic cancer.

1.2.2 Risk factors

Most patients are about 70 years old, both sexes being affected similarly. The main known risk factors for development of PDAC are tobacco smoking, obesity, exposure to certain chemicals, diabetes (especially new-onset type 2), chronic pancreatitis and family history (5). Most cases are sporadic, but about 10 % are linked to inherited mutations in genes such as BRCA1 or BRCA2 (hereditary breast and ovarian cancer syndrome), PALB2 (hereditary breast cancer), p16/CDKN2A (familial melanoma), FAMMM (familial atypical multiple mole melanoma syndrome), MLH1 or MSH2 (hereditary non-polyposis colorectal cancer, HNPCC), STK11 (Peutz-Jeghers syndrome), and PRSS1 (familial pancreatitis).

1.2.3 Precursor lesions

Evidence derived from morphological and genetic analysis of clinical samples and genetically engineered mouse models indicates that the development of PDAC follows a multistep process with progressive accumulation of mutations. These are reflected at the morphological level in premalignant lesions with an increasing grade of dysplasia (low grade > high grade) leading eventually to invasive adenocarcinoma. Two main types of precursor lesions are recognized (6,7) (Figure 1): the microscopic pancreatic intraepithelial neoplasia (PanIN) and the macroscopically evident mucinous cystic neoplasia and intraductal papillary mucinous neoplasia (IPMN), of which the latter is the most common and well characterized. The canonical neoplastic progression from low-grade PanIN starts with activating oncogenic mutation of the KRAS gen followed by mutation of CDKN2A and in high-grade dysplasia/PDAC additional mutation of TP53 and/or loss of SMAD4 (8). In contrast, IPMNs frequently harbor activating GNAS mutations (9).

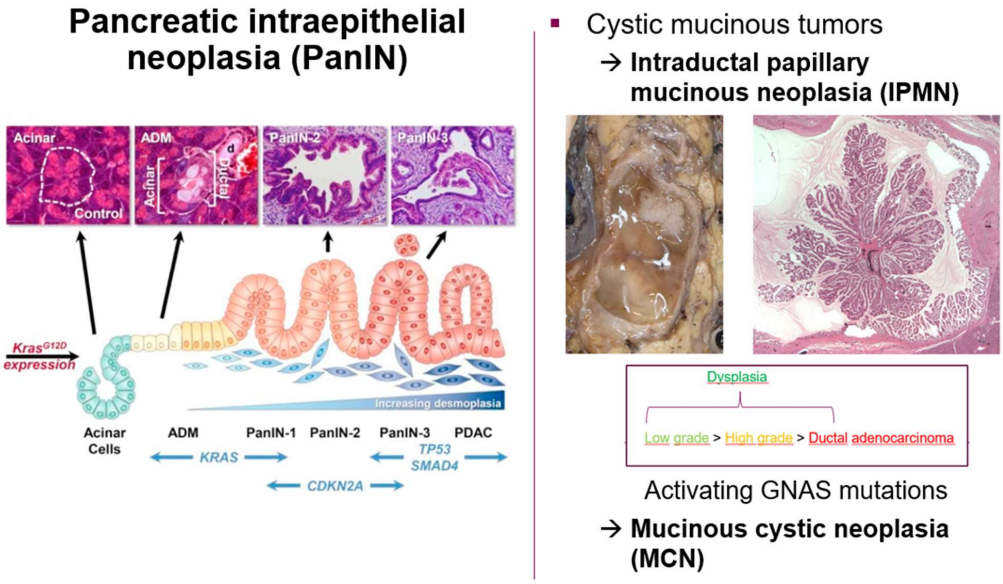

Figure 1 - Precursor lesions of PDAC. Left: From Han et al. Recapitulation of complex transport and action of drugs at the tumor microenvironment using tumor-microenvironment-on-chip. Cancer Lett. 2016;380:319-29. Copyright © 2015 Elsevier Ireland Ltd. All rights reserved. Right: Photographs courtesy of Prof. Caroline Sophie Verbeke.

1.2.4 Current treatment

PDAC is an aggressive type of cancer with a 5-year relative survival rate between 6 and 9 % in the United States all stages combined (10). The main reasons for the high mortality are a late diagnosis and pronounced resistance to treatment. The former is due to the absence of specific or sufficiently alarming signs or symptoms in early-stage pancreatic cancer (11) and the lack of specific, cost-effective and reliable screening tests (12). The most effective treatment is surgical removal of all or part of the pancreas, but unfortunately only about 20 % of patients are eligible for surgery (13). In 80 % of patients, the tumor is locally too advanced for surgical removal or has spread to the peritoneal cavity or distant

parts of the body such as the liver and lungs, precluding a survival benefit from surgery. Median survival without surgery is about 3.5 months, while this rises to 15–20 (14) and up to 30 (15) months for operated patients.

Patients are stratified for treatment according to tumor stage and performance status. The former is divided into the clinical categories of resectable, borderline resectable, locally advanced, and metastatic disease, while the latter is defined according to the Eastern Cooperative Oncology Group (ECOG) score.

2 LITERATURE REVIEW

2.1.1 Oncological treatment for pancreatic cancer

Adjuvant chemotherapy is routinely administered after surgery unless the patient cannot tolerate it. Gemcitabine (CONKO-001 trial) (16) or fluorouracil (5-FU) plus leucovorin (ESPAC-1 trial) (17) for six months have shown a survival benefit of about 10 % compared to patients who did not received chemotherapy. Until 2011, monotherapy with gemcitabine remained standard of care. More recently, the ESPAC-4 trial has demonstrated a superior estimated 5-year survival for combination treatment with gemcitabine and capecitabine (GemCap, 28.8 %) compared to gemcitabine only (16.3 %) (18), hence in Sweden, GemCap is currently recommended as standard chemotherapy in the adjuvant setting. With increasing frequency, neoadjuvant (preoperative) chemotherapy, often with the intensive FOLFIRINOX (folinic acid, fluorouracil, irinotecan and oxaliplatin) regimen, is administered with the objective to shrink a locally advanced or borderline resectable pancreatic tumor (19). Initial reports on the benefit of neoadjuvant therapy for borderline/locally advanced pancreatic cancer are promising but await confirmation in randomized controlled trials. Lately, a modified FOLFIRINOX regimen in the adjuvant setting (PRODIGE 24 trial) (20) has also been demonstrated to result in a significantly longer median disease-free survival (21.6 vs 12.8 months) and median overall survival (54.4 vs 35 months) among patients with resected pancreatic cancer, compared to gemcitabine only, albeit at the expense of a higher incidence of toxic effects.

Humble progress has also been made during the past years for the majority (80 %) of patients with inoperable disease, i.e., with distant metastases and/or local irresectability, who generally qualify for systemic palliative chemotherapy. Clinical trials have demonstrated a survival benefit for FOLFIRINOX (11.1 vs 6.8 months) (21) or nab-paclitaxel plus gemcitabine (8.5 vs 6.7 months) (22) versus gemcitabine only. However, both combination regimens are associated with substantial toxicity, mainly in the form of neutropenia, which limits their use to patients with good performance status without relevant comorbidities. This illustrates the urgent need for more effective medical treatment strategies, both for first- and second-line therapy, as most patients progress within a few months during or after first-line palliative chemotherapy. Novel therapeutic strategies are being investigated (23), including pathway inhibitors (ROS1, TRKA-B, and ALK fusions, MEK inhibitors), DNA repair (PARP inhibitors for BRCAness phenotypes), immunotherapy (PD-L1 and CTLA-4 checkpoint inhibitors, CAR T-cells), cancer cell metabolism (mitochondrial tricarboxylic acid cycle) and targeting of the extracellular matrix (hyaluronic acid). Unfortunately, most targeted therapies and immunotherapies have so far failed to improve survival, but future clinical trials that focus on defined subgroups of patients predicted to benefit from these treatments will hopefully overcome the disappointing results observed in unselected populations of patients with advanced pancreatic cancer.

2.2 THE TUMOR MICROENVIRONMENT (TME)

Human PDAC is characterized by the presence of a prominent desmoplastic and hypovascular stromal microenvironment that is composed of an admixture of acellular and cellular elements, including the extracellular matrix (ECM), mesenchymal cells (mainly

cancer associated fibroblasts, CAFs) and immune cells. The TME is a highly dynamic milieu in which a complex interplay and molecular signaling cross-talks develop in paracrine and autocrine manners with pleiotropic effects on all its components and the cancer cells (Figure 2).

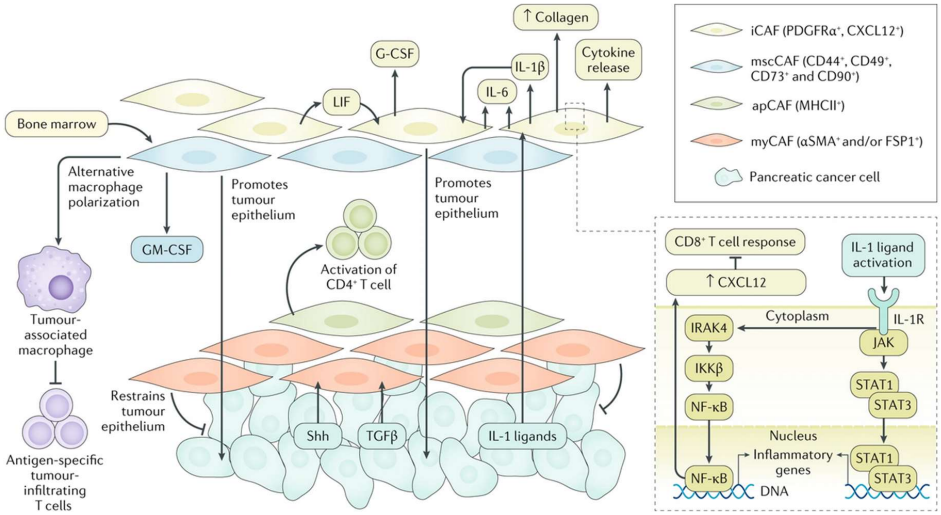

Figure 2 - The tumor microenvironment in PDAC. iCAF: inflammatory CAF. mscCAF: mesenchymal stem cell-derived CAF. apCAF: antigen presenting CAF. myCAF: myofibroblastic CAF. From Hosein et al. Pancreatic cancer stroma: an update on therapeutic targeting strategies. Nat Rev Gastroenterol Hepatol. 2020 Aug;17:487-505. Copyright © 2020, Springer Nature Limited.

For many years, the TME was regarded as a mere passive bystander. A first shift in the paradigm occurred by 2010, when the TME was recognized to have a tumor promoting role (24) supporting tumor growth and invasion, e.g., by overexpression of matrix metalloproteinases (MMPs, like MMP-2 and MMP-9) that degrade the surrounding ECM, or by overexpression of the serine protease inhibitor SERPINE 2 (25) that induces intensive ECM production rich in collagen type 1, fibronectin and laminin, resembling the desmoplastic reaction observed in PDAC.

Pancreatic stellate cells (PSCs) emerged as the most important mesenchymal cell type or CAF in the TME. PSCs are normally present in the periacinar stroma in a quiescent state and store vitamin A droplets. They shift to an activated state in response to cytokines and growth factors, like TGF-β, PDGF and FGF-2 that are secreted by inflammatory and cancer cells (26), or in response to oxidative stress, caused for instance by the toxic metabolites of ethanol in pancreatic acinar cells. Activated PSCs display a myofibroblast phenotype with high expression of α-smooth muscle actin (αSMA^+) and produce ECM components (collagen types 1 and 3, fibronectin, hyaluronic acid) and MMPs. Löhr et at. demonstrated that TGF-β1-transfected PDAC cells increased synthesis of extracellular matrix proteins including collagen type I on fibroblasts upon stimulation through cocultivation or conditioned media, and induced desmoplastic stroma reaction in a xenografted nude mouse model (27). The activation of PSCs enables the establishment of paracrine and autocrine secretion and signaling loops that perpetuate PSC activation, causing the development of

the prominent desmoplastic stromal reaction that is characteristic for PDAC. Activation of Hedgehog (HH) signaling through overexpression of HH ligands by cancer cells likewise results in activation of PSCs and promotes stromal desmoplasia (28).

Subsequent studies unveiled several tumor promoting effects of PSCs. Hwang et al. (29) showed that PSC-conditioned medium increased proliferation, migration, invasion and colony formation in a dose dependent manner in PDAC cell lines, and inhibited the effects of chemotherapy and radiation. Furthermore, another study supported a metastasis promoting role for PSCs, evidenced by a higher number of metastases in mice injected with PDAC cell line plus human PSCs compared to tumor cells only (30). Recently, a potential role of PSCs in the impairment of response to chemotherapy has been suggested, due to a selective scavenging and accumulation of activated gemcitabine metabolites in PSCs (31), which remain sequestered intracellularly and consequently are not made available to tumor cells.

Evidence regarding the active tumor promoting role of CAFs in the TME fueled the interest in targeting the stroma as a therapeutic approach for PDAC. The HH signaling pathway emerged as a clear candidate due to upregulation of the ligand in PDAC and its desmoplasia-promoting effect, but clinical trials on metastatic PDAC investigating the addition of HH antagonists to gemcitabine treatment were disappointing (32). Two clinical trials showed no benefit compared to gemcitabine alone (33,34), while a third one had to be interrupted due to decreased survival in the combination arm.

Two elegant studies in 2014 fostered a second shift in the TME paradigm. Using different approaches in genetically engineered mouse models, both studies showed that depleting the stroma is counterproductive as it indeed abolishes the previously unrecognized concomitant tumor restraining role of the TME. Rhim et al. (35) depleted PDAC tumors by deleting Sonic hedgehog (Shh) ligand, while Özdemir et al. (36) genetically deleted αSMA^+ myofibroblasts. In both cases the stromal content was reduced, but unexpectedly, this led to more aggressive, invasive, proliferating, and undifferentiated tumors and decreased survival. Tumors depleted of αSMA^+ myofibroblasts showed an increase in the epithelial-to-mesenchymal transition (EMT) programs, as evidenced by αSMA^+ cancer cells and enhanced transcriptional expression of the EMT genes TWIST, SNAIL and SLUG.

A third paradigm shift, partly driven by the groundbreaking advances of immunotherapy in other solid tumors like melanoma, lung cancer and mismatch repair (MMR) deficient colorectal cancer, was the full recognition of the immune microenvironment as a key element of the TME in PDAC and the crucial role of CAFs in governing local immune surveillance.

However, the immune microenvironment in PDAC has unique characteristics (37):

- In contrast to other solid cancers, which may display substantial lymphocytic infiltration, the number of intratumoral effector T-cells is low.
- The RAS oncogene is associated with activation of inflammatory pathways in which Cox2, IL-6 and its downstream effector phospho-Stat3 are overexpressed (38). This creates a persistent tumor-associated chronic inflammatory micromilieu.

- Infiltrates of myeloid derived suppressor cells (MDSCs) play a direct role in immune suppression, promoting unrestricted cancer cell growth.
- Finally, PDAC cells grow in an extensive and dense fibrous stroma that constitutes a barrier to the recruitment of immune cells.

The interplay between two fundamental immunological processes, the effector, and the suppressor, determines the immune response against cancer cells:

- Effector immune cells:
    - $CD8^+$ cytotoxic and $CD4^+$ helper T-cells - tumor infiltrating lymphocytes (TILs): TILs are the most important anti-tumor immune elements in the TME. High numbers of $CD8^+$ and $CD4^+$ T-cells are associated with a longer survival in PDAC (39,40), but their numbers are usually low, probably due to the effect of the stroma, CAFs (41) and suppressor immune cells. The $CD45RO^+$ memory $CD8^+$ T-cells are considered to be the major anti-tumor effector cells. Among $CD4^+$ cells, the effector Th1 cells ($Tbet^+$) activate antigen presenting cells, like dendritic cells, to potentiate the presentation of tumor antigens to cytotoxic T-cells. In contrast, Th2 cells ($GATA3^+$) have been suggested to induce tumor tolerance. Disproportionately high ratios of Th2 / Th1 have been reported in PDAC, associated with a reduced survival (42), indicative of an ineffective immune response against the cancer cells (43). Interestingly, the Th2 cell polarization was mediated by thymic stromal lymphopoietin (TSLP) secreted by CAFs, an observation that illustrates well the complex cross-talk between tumor cells, CAFs and immune cells in the TME.
    - Natural killer cells (NK): Are divided into two types.
        - *Type I (invariant)*: Recognize and eliminate cancer cells, mainly by binding of Natural Killer Group 2, member D (NKG2D) activating receptor to the ligand MHC class I chain A (MICA) that is expressed on epithelial tumors, including PDAC. But tumor cells can express and secrete into the serum sMICA, a cleaved product of MICA after proteolytic shedding. Higher serum levels of sMICA showed significant inverse correlation with NKG2D expression in NK cells and moreover, these were functionally impaired, not capable of killing PDAC cells (44). Evidence indicates that expression of sMICA by the tumor cells may represent an immune evasion mechanism that leads to the impairment of immunosurveillance by NK cells and/or CD8 cytotoxic- and γδ-T cells, which also express NKG2D.
        - *Type 2*: Promote tumor progression by producing IL-13, which in turn induces accumulation of MDSCs and/or polarizes macrophages towards the tumor-promoting M2-phenotype.

- Suppressor immune cells:
    - T-regulatory cells ($CD4^+$, $CD25^+$, $FoxP3^+$): Exert immunosuppressive activity through the release of cytokines, including TGF-β and IL-10. As previously noted, the ineffective form $CD4^+$ Th2 plays a major role in tumor tolerance.
    - Tumor associated macrophages (TAMs): Are divided into two phenotypes (45):
        - *M1 (classical) macrophages*: Highly inflammatory and effective in promoting activation of immune cells capable of killing cells. Generate high levels of pro-inflammatory cytokines such as IL-12 and low amounts of IL-10, which promotes the differentiation of $CD4^+$ T cells into Th1 cells and activated cytotoxic $CD8^+$ T cells.
        - *M2 (alternative) macrophages*: Inhibit inflammatory responses and adaptive Th1 immunity. Promote angiogenesis and tumor development. Generate low levels of IL-12 and high of IL-10.
        - Extensive TAM infiltration is generally associated with a poor prognosis in several human cancers. One important mechanism of tumor immune scape is through the expression of the programmed death ligand 1 (PD-L1) by macrophages that binds to PD-1, an inhibitory receptor that leads to induction of apoptosis in activated T-cells.
    - Myeloid derived suppressor cells (MDSCs): Comprise a heterogeneous population of immature myeloid cells precursors of dendritic cells, macrophages, and granulocytes (46). MDSCs are driven by tumor-secreted factors, in particular GM-CSF that promotes recruitment of myeloid progenitor cells and their differentiation into MDSCs. MDSCs perturb both the innate and adaptive ($CD4^+$ and $CD8^+$ T cell activation) immune responses and evidence indicates that are potent inhibitors of antitumor immunity in-vivo. Treatments that reduce MDSCs such as gemcitabine and surgical resection, which reduce the tumor mass, also contribute to restore immune surveillance and activate T and NK cells.
- Cancer associated fibroblasts:
    - Pancreatic stellate cells (PSCs): It has been suggested that PSCs play a role in regulating the immune response to the tumor (26). PSCs promote the differentiation of peripheral blood monocytes into MDSCs through activation of STAT3 signaling by PSC-derived IL-6 (47). Activated PSCs express high levels of galectin-1, which impairs survival of T cells (48). It has also been suggested that PSCs can attract and sequester $CD8^+$ T cells via the CXCL12/CXCR4 axis, reducing their migration to the juxtatumoral stromal compartment and impeding their contact with the tumor cells (49).

- FAP+ cancer associated fibroblasts (CAFs): These CAFs were found to contribute to an immunosuppressive TME and resistance to checkpoint antagonists in a GEMM of PDAC by production of the chemokine CXCL12 (50). Depletion of the FAP+ cells uncovered the antitumoral effects of anti-CTLA-4 and anti-PD-L1 drugs that otherwise failed in this model, while treatment with an inhibitor of the CXCL12 receptor CXCR4 induced T-cell accumulation around cancer cells and a synergistic antitumoral effect with anti-PD-L1.
- Pancreatic CAFs have also been shown to suppress T cell proliferation and proinflammatory cytokine release and to promote the expression of co-inhibitory markers, such as PD-1 and TIM-3, on activated T cells (41).

The latter studies highlight, in a subsequent shift of the TME's paradigm, the phenotypic heterogeneity of the stroma and CAF subpopulations and the need to gain deeper knowledge as a means to open the path for novel therapeutic approaches aimed at reprogramming rather than depleting the stroma and promoting the more tumor-restraining stromal phenotypes (32).

Following this line of investigation, a growing body of research describes several partially overlapping stroma subtypes based on transcriptional profiling or histomorphology that are associated with differences in prognosis:

- Erkan et al. (51) showed that the activated stroma index, determined as the the ratio of α-SMA (marker of PSC activity) to collagen (deposition) stained area, was an independent prognostic factor associated with a shorter survival.
- "Activated" vs "classical" (52):
  - "Classical" stroma: Is characterized by high numbers of PSCs expressing α-SMA, desmin and vimentin and associated with a more favorable survival (median 24 months).
  - "Activated" stroma: Proinflammatory, contains large numbers of macrophages, shows upregulation of chemokine ligands (like CCL13 and CCL18) and is associated with a shorter survival (median 15 months).
- "Mature", "intermediate", "immature" (53):
  - "Mature" stroma: Contains a dense amount of collagen fibers and low number of CAFs.
  - "Immature" stroma: Is highly cellular and collagen poor; was associated with a poorer survival.
  - "Intermediate" stroma: Between the mature and immature types.
- "(Highly) stiff" stroma (54): Defined by matricellular-enriched fibrosis with high tissue tension, was associated with reduced TGF-β signaling, elevated β-integrin mechano-signaling and epithelial STAT3 activation, resulting in accelerated tumor progression and shortened survival.

Evidence indicates that different CAF subpopulations determine the diverging stroma subtypes (55–59):

- Several "general" CAF markers have been identified, like collagen type I alpha 1 chain, fibroblast activation protein alpha (FAP-α), vimentin, decorin and podoplanin (D2-40).
- "Myofibroblastic" CAFs: Tumor restraining. Located immediately adjacent to and surrounding the cancer cell clusters. These are induced by tumor-secreted TGFβ and activation of the TGFβ / SMAD2/3 pathway in CAFs. Show high α-SMA expression, active HH signaling and upregulation of pathways related to smooth muscle contraction, focal adhesion, ECM organization, collagen formation and promotion of mesenchymal phenotype.
- "Inflammatory" CAFs: Tumor promoting. Located more at a distanc from the cancer cells, distributed throughout the tumor field. Induced by tumor secreted IL-1/JAK-STAT3 pathway activation in CAFs. Show low α-SMA and secrete inflammatory cytokines such as IL-6, IL-11 and LIF, chemokines, matrix remodeling proteins and growth factors. Inflammatory CAFs show upregulation of inflammatory pathways such as IFNγ response, TNF/NF-κB, IL2/STAT5, IL6/JAK/STAT3, and complement. Exhibit specific expression of hyaluronan synthases (HAS1, HAS2). Hyaluronan, a major component of the ECM, has been identified as a major source of solid tumor stress impairing vascular perfusion and compromising drug delivery. Transcriptomic analysis revealed type 1 receptor for angiotensin II as a marker of inflammatory CAFs, which could be associated with the reduction in solid stress and improved survival observed in murine models of PDAC following treatment with Losartan, an inhibitor of this receptor (60,61), which is currently being investigated as part of combination treatment in clinical trials (NCT01821729, NCT03563248).
- Öhlund et al. showed that PSCs plated in Matrigel induced quiescent PSCs and that these could transdifferentiate either into inflammatory CAFs when co-cultured with PDAC organoid-conditioned medium or into myofibroblastic CAFs when cultured in two-dimensional monolayers (57). Remarkably, the CAF phenotypes were mutually exclusive but dynamically reversible according to the culture conditions, indicative of phenotypic CAF plasticity. Along with this line, a recent study by Liu et al. (62) performed comprehensive transcriptomic analyses in a 3D spheroid model of PSC and PDAC. They showed than when co-cultured in heterospheroids, PSCs shifted from myofibroblastic to inflammatory CAF phenotype, while PDAC cells did from a classical/progenitor to a basal-like/squamous subtype, and their sensitivity to gemcitabine was increased.
- "Antigen presenting" CAFs: Single cell transcriptomic analysis of human and murine PDAC revealed the presence of a further distinct CAF subpopulation that expresses MHC class II and CD74, but not classical co-stimulatory molecules, suggesting that they contribute to the immune suppressive microenvironment by inducing anergy or Treg differentiation of CD4+ T cells (55).

Another subtype of CD10+ CAFs was previously described, with increased secretion of matrix metalloproteases and associated with enhanced cancer progression (63). It is expected that additional subpopulations of CAFs will be described in future studies as well as potential therapeutic approaches targeting pro-tumorigenic signaling pathways in CAFs.

In this context, much of the research on PDAC-stroma interactions and stroma targeting relies on in-vitro studies with (co)cultures of PSCs. As shown by Lenggenhager et al. (64) PSCs from different origins and conditions (human/murine, primary/immortalized, from normal pancreas/chronic pancreatitis/PDAC) show diverging phenotypes and functional traits, such that selection of the most suitable and biologically relevant PSC must be considered carefully based on the specific research questions and experimental setting.

2.3 MORPHOLOGICAL HETEROGENEITY IN PANCREATIC CANCER

Morphological diversity is a prominent but barely investigated feature of PDAC (65). It presents both at inter- and intratumoral levels and is likely to reflect key biological features of the cancer cells and the tumor microenvironment, such as mutational landscape, epigenetic alterations, and distinct cross-talks in the diverse stromal compartments, like the pancreatic stroma, duodenal wall, peripancreatic fat tissue, perineural space, and lymphatic and blood vessels. Ligorio et al. (66) demonstrated functionally and analytically the influence of the stroma on shaping glandular composition in PDAC with respect to epithelial-mesenchymal transition (EMT) and proliferative (PRO) cancer cell phenotypes. The cancer cells were dominated by a double negative EMT-/PRO- phenotype when cultured in absence of CAFs, shifted towards EMT+ and PRO+ phenotypes when cocultured with CAFs and peaked in double positive EMT+/PRO+ cancer cells when CAFs outnumbered the cancer cells in coculture. EMT and PRO phenotypes were linked to activation of MAPK and STAT3 signaling pathways in the cancer cells and secretion of TGF-β1 by the CAFs. Investigation of a clinical cohort of primary PDAC showed, in line with the preclinical results, that glands dominated by double positive EMT+/PRO+ cells were enriched in tumors with high stroma content, EMT+ containing glands in tumors with medium stroma content, and PRO+ glands in tumors with low stroma. In a recent study, Sántha (67) et al. described four common patterns of pancreatic cancer (periglandular, tendon-like, fascicular, and chickenwire) with distinctive morphological configurations and (immuno)-histochemical features of the tumor glands and their respective cancer-associated stroma. These findings further support a correlation of morphological heterogeneity with structural and functional diversity in pancreatic cancer.

Although the complete spectrum of morphological diversity in PDAC is not yet fully catalogued, it is partly reflected in the WHO classification (68). The latter roughly distinguishes between “subtypes” and “patterns”, where only the former ones are encouraged to be reported by pathologists, as these have been associated with differences in prognosis and may harbor different molecular signatures. Noteworthy, most of the morphological subtypes and patterns were described mostly on a morphological basis, in single studies, on small cohorts, between 1984 and 2012, and have not been further revised or followed up by continuation studies.

The PDAC subtypes include anaplastic (69), adenosquamous (70), hepatoid (71), medullary (72), undifferentiated with osteoclast-like giant cells (73), signet ring (74), colloid (75), and invasive micropapillary (76). Among them, the anaplastic, adenosquamous and hepatoid subtypes have been associated with a worse prognosis, while a fraction of medullary

carcinomas are MMR-deficient and may be associated with hereditary nonpolyposis colorectal cancer (HNPCC) or EBV infection.

Described PDAC patterns include large duct (77), foamy-gland (78), clear cell (HNF-1β+) (79), microcystic/vacuolated (80), paucicellular infiltrating (81), and cystic papillary (82). As their reporting is not included in the current pathology guidelines, the incidence and potential prognostic and therapeutic implications are largely unknown. Reporting of histological subtypes is also challenging due to intratumoral heterogeneity and co-occurrence of multiple subtypes in the same tumor, histomorphologies that do not fit in the described categories above, the inherent difficulty of manually quantitating histological components by light microscopy, sampling bias, and the lack of established systems for scoring/assessment.

More thoroughly studied is the impact of an intestinal versus pancreatobiliary type of differentiation in adenocarcinomas from the periampullary region, including PDAC. The intestinal subtype, whose morphology resembles that of colorectal cancer, was first described in PDAC by Albores-Saavedra et al. (83). It is composed of tubular, simple/branching/cystically dilated glands with foci of cribiform structures. Intestinal-type tumor cells are tall columnar, with a variable amount of cytoplasmic mucin and admixed collections of goblet cells. Nuclei are typically ovoid/elongated, hyperchromatic/vesicular and pseudostratified. By contrast, conventional pancreatobiliary-type adenocarcinoma grows in simple/branching glands and small, solid tumor cell nests. The cells are cuboidal/low columnar and single layered. The nuclei are round, with marked variation in size and shape and lack pseudostratification. However, “mixed” and “hybrid” histomorphological features can hamper reproducibility and definite tumor subtyping (84).

Immunohistochemical staining is helpful to distinguish between intestinal and pancreatobiliary type tumors (85,86). Intestinal-type adenocarcinomas express CK20, MUC2 and CDX2, while those of the pancreatobiliary type are immunoreactive for CK17, MUC1, MUC4, MUC5AC, CA19-9 and CA125. However, a fraction of periampullary adenocarcinomas may show also at the immunohistochemical level “mixed” immunoprofiles.

Multiple studies have shown that periampullary adenocarcinomas of the intestinal type, and in particular those arising from the ampulla of Vater, have a better prognosis than those of the pancreatobiliary type (85,87,88). Interestingly, a number of studies (87,88) found that the histological type of differentiation, rather than the primary tumor location, was an independent predictor of survival on multivariate analysis. Altogether, evidence indicates that intestinal and pancreatobiliary tumors potentially represent distinct diseases with therapeutic implications and that the histological type of differentiation should be accounted for when interpreting past clinical trials and for future trial design (89).

2.4 MOLECULAR HETEROGENEITY IN PANCREATIC CANCER

PDAC is presently recognized as a heterogenous disease and efforts to establish molecular subtypes that predict therapeutic responses and guide clinical decision making are currently under intensive investigation (90). A large integrated genomic analysis with histopathological correlation (91) identified four subtypes: squamous, associated with the adenosquamous variant of PDAC; pancreatic progenitor; immunogenic, associated with upregulation of immune networks, including acquired immune suppressive pathways; and aberrantly differentiated endocrine-exocrine. In another study, Moffit et al. (52) identified

based on gene expression analysis two subtypes of PDAC: (i) a classical (pancreatic) subtype, characterized by upregulation of genes like CEACAM6 and KRT20, associated with a better survival, and (ii) a basal-like subtype, that is characterized by upregulation of KRT17, KRT15, KRT6A, SERPINB3 and S100A and associated with a significantly worse overall survival. Recently, Chan-Seng-Yue et al. (92) performed whole genome and bulk transcriptome analysis in a large cohort of resectable (stage I/II) and advanced (stage III/IV) PDAC. Both subtypes were subdivided further into categories A and B. Classical-A/B tumors were characterized by upregulation of transcription factors related to pancreatic lineage differentiation, like GATA6, HNF1A and HNF4G, and were more frequent in early stage (I/II). The classical-A subtype showed lower frequency of intact SMAD4. Basal-like subtypes, in which expression of classical transcription factors is lost, showed a diverging distribution, being basal-like-A more frequent in stage IV (metastatic disease) and associated with a high chemoresistance; while basal-like-B was more frequent in early stage (resectable). Single cell RNA-seq, performed in a subset of tumors, showed that both basal-like and classical cell populations often co-exist in different proportions within the same tumor, creating a transcriptional continuum at the bulk transcriptome level. Kalimuthu et al. (93) assessed a series of resected PDAC with matched transcriptome data and classified them into two morphological categories, ‘gland forming’ (comprising conventional and tubulopapillary) and ‘non-gland forming’ (comprising composite and squamous). Guided by transcriptome data, a cutpoint of 40 % gland formation was chosen to divide the tumors into these two groups, which correlated with the classical and basal-like molecular subtypes and differed in overall survival. This study supports the possibility of linking the established molecular subtypes with morphology-based assessments, which are easier to be adopted into routine clinical practice.

Several molecular classification systems have been proposed. Very recently, the division into two categories have been challenged by studies that show marked intratumor heterogeneity, such that a “molecular gradient” rather than discrete molecular categories has been proposed (94).

Molecular classifiers for prediction of response to therapy in the context of precision medicine are also beginning to emerge. In a comprehensive multicenter study, Tiriac et al. (95) generated a large library of PDAC patient derived organoids, which allowed the evaluation of responses to a panel of chemotherapeutic drugs (“pharmacotyping”). In addition to classifying the patient derived organoids into classic and basal-like subtypes, transcriptomic analysis identified a gemcitabine-sensitivity signature that stratified patients according to response status to adjuvant gemcitabine.

2.5 EX-VIVO ORGANOTYPIC SLICE CULTURE

Cultured tissue slices have been used since 1923 for studies on liver metabolism or transport processes in the kidney and became more widespread as an in-vitro tool to study metabolism and toxicity in various organs after the introduction of the Krumdieck tissue slicer. Tissue slicers allow the production of precision-cut tissue slices of a consistent thickness with minimal cutting-induced damage (96). The cultured tissue slices can then be submitted to any possible analytical method.

When it comes to cancer, during the past decade a progressively growing body of literature has used precision-cut tissue slices from different tumor types to address key questions

related to oncogenic signaling pathways (97), intratumoral heterogeneity, drug sensitivity testing and immunotherapy. The main advantages of the tissue slices, in contrast to traditional cell cultures (2D, 3D, organoids), xenograft-based or genetically engineered mouse models are the preservation of the native tumor microenvironment and the 3-dimensional tissue architecture that render this model a close surrogate to the parent tumor. The biological relevance of the 3D tumor configuration and the reciprocal influences with the stroma has also been highlighted by in-vitro studies on cell lines. Our group showed that PDAC cell lines cultured as 3D spheroids versus in 2D showed upregulation of extracellular matrix and chemoresistance related genes, as well as increased resistance to a panel of drugs, including gemcitabine (98). In a continuation study, PDAC cells co-cultured with PSCs in 3D spheroids demonstrated increased proliferation and shift towards a more mesenchymal phenotype, while PSCs showed activation and shift towards a myofibroblast phenotype, as compared to spheroid monocultures (99).

The ultimate goal of the slice culture is to mimic as closely as possible the in-vivo situation as a means to narrow the current enormous gap between preclinical and clinical results and hence be able to predict drug responses in a reliable and reproducible way. These features render the slice culture a state of the art low-throughput but high-content experimental platform for drug testing and investigation of tumor biology.

2.5.1 General workflow for ex-vivo organotypic slice cultures in the literature

Soft and fatty tissues, such as breast tissue, were previously embedded in low melting point agarose to improve the success rate of the slicing process (100). Slicing was performed using a vibrating blade microtome (Leica VT, Krumdieck) or a tissue chopper (101). Typical culture time was about one week. Tissue slices were most often cultured at atmospheric condition (21 % O_2), with 5 % CO_2 and at 37 °C (97). Systematic optimization procedures identified the use of semipermeable inserts as an important factor to improve tissue viability. After harvesting, preservation of the native tumor histomorphology was assessed by light microscopy and comparison with the non-cultured/parent tumor. Tissue viability during culture and cancer cell viability after drug exposure were assessed by combination of morphology-based techniques and biochemical assays. Morphological techniques and molecular analyses were used for the assessment of signaling pathways (102).

2.5.2 Organotypic slice cultures of the pancreas

Pancreatic studies based on precision-cut tissue slices have focused mainly on investigating the transfection efficacy for viral-vector-mediated gene therapy (103), stress-mediated activation of PSCs (104), and physiology of acinar cells and islets of Langerhans (105). Recently, our group has published a study (106) presenting an optimized protocol for culturing precision-cut tissue slices from human PDAC during at least 4 days with subsequent thorough histomorphological and immunohistochemical characterizations of the tumor cells and the tumor microenvironment. We showed that the grade of tumor differentiation remained unaltered during culture inclusive in a progressive cell outgrowth occurring on the surface of the tissue slices, and that proliferation was maintained.

When it comes to therapeutics, Jiang et al. (107) showed viability and preservation of the tumor, stroma and immune microenvironment in precision-cut slices of human PDAC for up to 6 days. Recapitulation of the cytotoxic effects of drug treatment was demonstrated by

exposing the tissue slices to staurosporine, a protein kinase inhibitor and inductor of apoptosis, and cycloheximide, an inhibitor of protein biosynthesis. After 48 h of treatment, the percentage of $Ki67^+$ cells was slightly decreased, while the total number of nuclei (cellularity) was diminished and the percentage of cleaved caspase-3 cells markedly increased, as assessed by brightfield immunohistochemistry. Cytotoxic effects to treatment were time- and dose-dependent. The three-dimensional spatial relationship between live-stained $EPCAM^+$ tumor cells and $CD8^+$ cytotoxic T-cells or fibronectin and $CD11^+$ macrophages could be imaged after fixation by confocal microscopy. Migration of autologous CFSE-labelled splenocytes into co-cultured tissue slices was also demonstrated.

In another study based on live and time-lapse fluorescent microscopy, Seo et al. (108) demonstrated reactivation, expansion, mobilization and tumor cell killing by resident $CD8^+$ T-cell clones in tissue slices of human PDAC following combination treatment with anti-PD1 and anti-CXCR4 antibodies. Supernatant from cultures showed presence at base line of CXCL12, the soluble ligand of CXCR4, which has been associated with an immunosuppressive microenvironment in multiple carcinoma types; and granzyme B and IFNγ effector molecules after combination therapy, suggesting active tumor cell killing. Combination treatment induced migration and relocation of $CD8^+$ T-cells into the juxtatumoral stroma containing $EPCAM^+$ cells. This was associated with a marked increase in tumor cell apoptosis, evidenced by SR-FLICA labeling of activated caspase-3 and -7 enzymes. The presence of clonally expanded T-cells within the PDAC microenvironment together with the synergistic effects of combined PD-1 and CXCR4 blockage argues against the concept of PDAC being an immunologically “cold” tumor. Rather, it supports the important role of the stroma in the sequestration and inactivation of tumor-reactive T cells and highlights the future prospect of developing effective immunotherapies against PDAC and other tumors showing immune exclusion.

2.5.3 Methodological aspects of ex-vivo tissue slice cultures of tumor types other than pancreas

Tissues slices have been used to investigate drug effects in breast cancer (100,109), glioblastoma (101,110), head and neck squamous cell carcinoma (111,112), gastric-esophagogastric junction cancer (113), and lung cancer (114).

Ex-vivo tissue slices allow testing of both simple and complex chemotherapy treatments, albeit with a single dose retaining the clinical ratio of its components. The optimal doses for ex-vivo experiments can be determined according to turning points for toxicity that have been established in previous cell culture experiments testing various concentrations and lengths of continuous drug exposure (109). Targeted drugs, like KRAS signaling inhibitors, have also successfully been investigated in tissue slices, where the cytotoxic drug responses correlated with the spatial signaling heterogeneity of the targeted pathways as assessed by immunohistochemistry (114).

Relevant readouts for evaluation of drug effect when comparing matched treated and untreated tissue slices were tumor cell content (112,114), tumor cell proliferation, cell death, and functional assays of cell viability like WST and ATP-utilization (112). Tumor cell content can be evaluated as the percentage of the tumor cell area with respect to the tissue slice. A pathologist can manually annotate non-viable tissue areas in digital histological slides. In addition, relative decrease in viability (expressed as percentage) can be calculated according to the formula: (1 – viability in drug treated / viability in untreated

control) * 100. The cytotoxic drug effect can then be plotted with a line representing the % of viable area in treated vs untreated slices (114). Tumor cell proliferation is commonly assessed by Ki67 immunostaining, which can be combined with CK19 or vimentin for a more precise discrimination between cancer cells and stroma/immune cells. Alternatively, immunofluorescence for EdU incorporation allows real time measurement of DNA synthesis. Cell death is detected on routine histology by the appearance of distinct nuclear and cytologic changes: karyolysis, pyknosis, karyorrhexis and apoptotic bodies. However, its quantification may require the use of special labelling techniques like TUNEL, γH2AX (immunohistochemistry, DNA double strand breaks) (115), cleaved cytokeratin 18 (M30) or activated caspase-3 (116). Propidium iodide (PI) can also be used to label necrotic cells on immunofluorescence.

Ex-vivo cultured tumors can then be classified into responders and non-responders to specific drugs according to the assessed readouts. Combining readouts from different levels (cell viability, histomorphology, proliferation and apoptosis) may increase the robustness of the classification and prediction models.

The predictive ability of slice culture for testing cytotoxic and targeted therapeutics can ultimately be validated by correlating the effects (according to readouts) in the tissue slices with the responses observed in human tumor-derived xenotransplants and in patient cohorts (112).

2.6 SELENIUM COMPOUNDS AS POTENTIAL CHEMOTHERAPEUTIC DRUGS

Selenium is an essential micronutrient found in many food sources, mainly breads, grains, meat, poultry, fish, and eggs (117). In adults, its daily requirement and upper safe levels of intake are 55 µg and 400 µg, respectively (118). Selenium deficiency is linked to a juvenile type of cardiomyopathy (Keshan disease) (119), while excess intake is toxic and can cause skin, neurological and gastrointestinal symptoms. Selenium is a key component of the family of selenocysteine (amino acid) containing selenoproteins. These play important roles in cellular antioxidant defense, redox homeostasis, male fertility, and thyroid function (120).

Redox-active selenium compounds are interesting candidate treatments for PDAC, as it has been shown by our group and others (121) that cancer cells, and in particular those that show resistance to conventional chemotherapeutics, are specifically sensitive to pharmacological modulations of redox states.

Cancer cells have an altered redox status that is characterized by higher rate of ROS production. This results in hyperactivation of pro-tumorigenic signaling pathways including proliferation, survival, and metabolic adaptation to the microenvironment. At the same time, higher ROS levels are toxic and can trigger cell death, senescence and proliferation arrest, such that cancer cells rely on higher levels of antioxidant proteins to maintain redox homeostasis (122). This, so called antioxidant response element (ARE) (123), induces proteins that mediate cellular detoxification and protection from oxidative stress, but also are associated with the development of resistance to conventional chemotherapeutic drugs. This

occurs e.g. by induction of multiresistance proteins (MRPs) and X^-_c cystine/glutamate antiporter expression that increases intracellular glutathione (GSH) levels (124).

Selenium compounds show high uptake in the pancreas, liver and kidney after oral administration (125). Sodium selenite (Se), an inorganic form of selenium, was previously shown that exerts a cancer-specific cytotoxic effect against different malignant cell lines and in particular against drug-resistant tumor cells (126,127). The tumor-selective cytotoxicity of Se is mediated by a high-affinity uptake of a reduced form of Se that is increased by X^-_c cystine/glutamate antiporter and MRP activity, together with highly increased oxidative stress due to redox-cycles of low-molecular-weight selenolates with intracellular thiols and oxygen. These cycles, sustained by intracellular glutathione (GSH) or the thioredoxin system, are very efficient and produce high levels of ROS that can overcome redox homeostasis and induce cytotoxic cell death in the cancer cells (128).

In contrast, methylselenocystein (MSC), an organic form of selenium, is biologically inert and can be considered as a pro-drug. MSC is metabolized in several organs including the pancreas and liver by the enzyme kynurenine aminotransferase 1 (KYAT1) into monomethylselenol (β-elimination product) and β-methylselenopyruvate (transamination product) (129). Monomethylselenol is highly redox-active and has been shown cytotoxic, antiproliferative, and proapoptotic properties in different malignant cell lines (130,131). While the α-keto acid metabolite β-methylselenopyruvate was reported to exert anti-tumor effects through inhibition of HDAC activity (132,133), which promotes proliferation, invasion and resistance to gemcitabine in pancreatic cancer cell lines through histone modifications (134). It has been further suggested that combination of MSC with an α-keto acid like phenylpyruvic acid (PPA) or indole-3-pyruvic acid (IPA) may have a synergistic effect and potentiate the cytotoxicity of MSC by increasing its β-elimination and reducing its transamination by KYAT1 (135).

Our group has carried out a phase I clinical trial where selenite was administered intravenous to cancer patients refractory to cytostatic drugs (136). Selenite was found to be safe and tolerable at dose levels up to 10.2 mg/m^2.

3 RESEARCH AIMS

Pancreatic ductal adenocarcinoma (PDAC) has a dismal prognosis with an overall 5-year survival < 9 %. Despite increasing knowledge regarding the biology of PDAC, improvement of treatment efficacy has been disappointingly small over the past decades. Two factors that likely may have hampered therapeutic advances are the traditional concept of PDAC as a homogenous disease and the limitation of experimental models for drug discovery to cell lines and xenograft mouse models, which only to a limited grade mimic human PDAC.

The overall aims of this thesis were to advance the field by addressing these questions, by (i) investigating tumor subtypes at the immunohistochemical level and analyzing the association with patient survival, and by (ii) establishing a novel, ex-vivo experimental model based on precision-cut tissue slices of human pancreatic cancer as a close surrogate for the parent tumor.

Thus, the specific aims for the individual studies were as follows:

1. To develop an integrative immunohistochemical classification of adenocarcinomas of the pancreatobiliary system to improve diagnosis and prognostic stratification. To specifically investigate the immunohistochemical diagnosis and prognostic significance of the intestinal and pancreatobiliary adenocarcinoma subtypes.
2. To establish an ex-vivo, precision-cut tissue slice model of human PDAC, to optimize culture conditions for keeping slices viable for at least 96 h, and to investigate the structural and functional integrity of the constituting neoplastic and non-neoplastic tissues by morphology-based techniques.
3. To further characterize the established precision-cut tissue slice model of human PDAC at the whole transcriptome level and investigate the value of transcriptomic analysis for the evaluation of the level of preservation of the tissue slices.
4. To investigate the use of the established precision-cut tissue slice model of human PDAC for drug sensitivity testing, and specifically, to investigate the potential of selenium compounds as a novel class of cancer chemotherapeutics.

4 MATERIALS AND METHODS

Work 1 ("*Immunohistochemical Typing of Adenocarcinomas of the Pancreatobiliary System Improves Diagnosis and Prognostic Stratification*") was a retrospective observational cohort study. The series comprised patients who underwent diagnostic core needle biopsy or surgical resection at Karolinska University Hospital between the years 2002 and 2013 for primary adenocarcinoma in the pancreatobiliary system, including PDAC, ampullary carcinoma, distal bile duct cancer, perihilar cholangiocarcinoma, and intrahepatic cholangiocarcinoma. A series of hepatocellular carcinomas were also included as a control group. The study included adenocarcinomas and histological variants, as defined by the World Health Organization (WHO) classification 2010 (137). However, adenosquamous carcinomas were excluded, to avoid excessive study complexity.

A total of 409 tumor samples from 370 patients were analyzed. For each sample, a representative block was stained with a comprehensive panel of immunohistochemical markers that are widely used in diagnostic pathology, according to established clinical diagnostic routines at Karolinska University Hospital. The panel for analysis comprised up to 27 immunohistochemical markers, including intermediate filaments (CK5, CK7, CK17, CK18, CK19, CK20, vimentin), mucins (MUC1, MUC2, MUC5AC, MUC6), markers usually expressed in adenocarcinomas of gastrointestinal and pancreatobiliary origin (BerEP4, EMA, CEA, CA19-9, CA125, maspin, CDX2), CD56, tumor suppressors (P53, SMAD4) and proliferation (Ki67). Immunohistochemical staining was scored quantitatively according to the percentage of positively stained tumor cells by visual assessment. Clinicopathological and outcome data were retrieved from the hospital medical records.

An omics-type bioinformatic analysis was performed using R software for statistical computing (version 3.0.2), the main steps being: data preprocessing, unsupervised clustering (hierarchical and complex network based), differential expression analysis, graphical visualizations (immunohistogram and complex network based), internal model validation, and survival analysis. Complex networks were generated using Gephi (version 0.8.2-beta). For differential expression, only the markers that were found to be significant by three different non-parametric methods, RankProd, SAM, and MultTest, were considered. An overview of the data analysis pipeline is shown in Figure 3. Internal model validation was based on machine learning classifiers using Weka (version 3.6.9). Survival analysis for mortality was performed using Kaplan–Meier curves and univariate (crude) and multivariate (adjusted) Cox proportional hazards regression models with p-values, hazard ratios (HR) and 95 % confidence intervals (CI). In multivariate analysis, the immunohistochemical or anatomically based tumor types were adjusted for tumor stage (pT) and lymph node status (pN). The Cox models' proportional hazards assumption was tested. The complete dataset, R code and reproducible computer environment for the analysis are provided on-line (http://dx.doi.org/10.5061/dryad.g8h71).

Figure 3 - Schematic overview of the data analysis pipeline. From Fernández Moro C et al. Immunohistochemical Typing of Adenocarcinomas of the Pancreatobiliary System Improves Diagnosis and Prognostic Stratification. PloS One. 2016;11:e0166067. Copyright © 2016 Fernández Moro C et al. CC-BY.

Work 2 ("*Ex-Vivo Organotypic Culture System of Precision-Cut Slices of Human Pancreatic Ductal Adenocarcinoma*") was a prospective preclinical experimental study. PDAC tumor samples from 12 chemonaïve patients operated at Karolinska University Hospital were cultured, comprising 4 well differentiated, 6 moderately-to-poorly differentiated and 2 non-gland forming, poorly differentiated carcinomas.

Fresh tumor tissue samples, between 5 and 10 mm in size, were obtained from surgical specimens immediately following resection. While being submerged in ice-cold medium, the tissue was cut into 350 µm thick tissue slices with the use of a vibrating blade microtome. The slicing procedure took on average 45 to 60 minutes and yielded between 12 and 17 slices per sample. The first slice (non-cultured, control, time point 0 h) was immediately fixed in formalin, and thereafter embedded in paraffin and processed for histology.

Optimal culture conditions were determined by following a systematic evaluation of several media, supplements, oxygen tensions and the use of inserts in preliminary experiments at the inception of the study. These indicated better viability of the tissue slices in CMRL medium supplemented with 2.5 % human serum (type AB, Sigma-Aldrich), 25 mmol/L HEPES, 1 mmol/L sodium pyruvate, 3 nmol/L zinc sulfate, 1X insulin-transferrin-sodium selenite solution, 1X PenStrep, and 100 nmol/L diphenyl diselenide (antioxidant). Slices were cultured at 37 °C in a humidified incubator for at least 96 h. Slices were rested on an organotypic insert (Millipore, 0.4 µm pore size) placed in a 35 mm culture dish containing 1.1 ml culture medium with a small volume (0.55 ml) of medium on top to prevent the tissue from drying out. Nine tumors were cultured under hyperoxic (41 % O_2) conditions and three under both hyperoxic and atmospheric (21 % O_2) conditions. Every 24 h, duplicate slices were harvested, embedded in paraffin, and processed for histology. The workflow for tissue slice preparation, culture and analysis is shown in Figure 4.

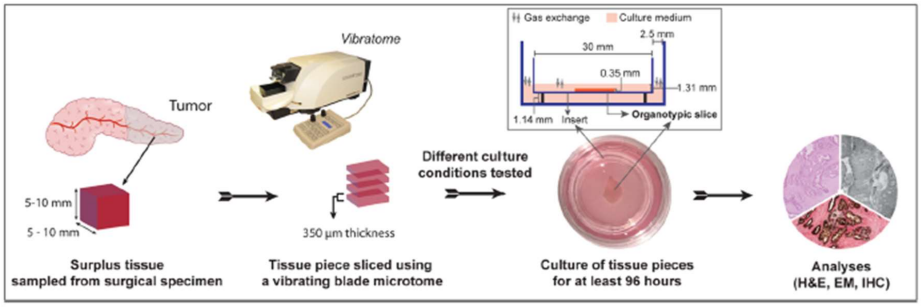

Figure 4 - Schematic representation of the workflow, including preparation, culture, and analysis of precision-cut tissue slices of human PDAC. From Misra S et al. Ex vivo organotypic culture system of precision-cut slices of human pancreatic ductal adenocarcinoma. Sci Rep. 2019 Feb 14;9:2133. Copyright © 2019, Misra S et al. CC-BY.

Hematoxylin and eosin (H&E) stained sections from the tissue slices were digitalized at 20X magnification. The digital slides were used for histomorphological assessments, including evaluation of the histological grade of differentiation, and quantification of tissue viability and cell outgrowth based on manual annotations and numeric processing of the annotation data using R. Main readouts were (i) the percentage of the entire tissue slice area showing damage (necrosis, apoptosis) and (ii) the percentage of the total perimeter of the tissue slice that was covered by either cancerous or non-neoplastic cell outgrowth. Quantitations were averaged over duplicate slices for each culture and time point (0 h, 24 h, 48 h, 72 h, and 96 h). Ultrastructural integrity was assessed by transmission electron microscopy in three cultures at 0 h, 24 h and 72 h. Immunohistochemical staining was performed using an automated immunostainer with a panel of markers to distinguish between epithelial, ductal/acinar, cancerous/non-neoplastic cell populations (CK7, CK18, CK19, trypsin, CA19-9, maspin, P53, SMAD4); to identify stromal cells (vimentin, α-SMA, D2-40, CD34), immune cell lineages (CD3, CD20, CD68), proliferating cells (Ki67); and to assess metabolic activity (pS6 mTOR pathway). Proliferative activity (Ki67-index) was assessed on all slices from seven cultures by manual annotation in hot-spots using

ImageJ (version 1.50i). Expression of stromal and immune cell markers and pS6 in cancer cells was quantified by digital image analysis using QuPath (version 1.3).

Comparisons of tissue viability, cell outgrowth, and proliferative activity between time points were performed using the Friedman test or Wilcoxon paired signed-rank test between matched cultures under hyperoxic and atmospheric O_2 conditions. Dunn's test was employed for multiple comparisons correction. A p-value of < 0.05 was considered statistically significant. Data analyses were performed using GraphPad Prism (version 6) and R (version 3.4.3).

Work 3 ("*Genome-wide Transcriptome Profiling of Ex-Vivo Precision-Cut Slices from Human Pancreatic Ductal Adenocarcinoma*") was a continuation study for the molecular characterization of the cultured tissue slices in Work 2. Hence, this was a retrospective study on tissue material from previously published tissue slice cultures of human PDAC. Criteria for inclusion were balanced grades of differentiation in the study series and availability of sufficient tissue material for analysis. Among duplicate slices, the one with higher tumor tissue content was selected. Five tissue slice cultures were included in the study, comprising two well differentiated, one moderately differentiated and two moderately to poorly differentiated carcinomas. For each culture, 0 h, 24 h, 48 h and 72 h time points were investigated.

The corresponding formalin-fixed paraffin-embedded tissue slice blocks were sectioned (2 × 10 µm curls). Subsequently, total RNA was extracted and cDNA whole transcriptome sequencing libraries were prepared using the Takara Smarter total-RNA Seq kit V2 Pico Input Mammalian (Takara Bio Inc). Ribosomal cDNA sequences were cleaved in the process. Both extracted RNA and generated libraries were quantified using respective Qubit 4.0 HS Assay Kits (Thermofisher Scientific). A total of twenty normalized libraries were sequenced using a NextSeq 500 Illumina system with High Output V2 Kit, generating a median of 40 million raw paired-end reads/sample. Processing and analysis of sequencing data were performed using the open source Chipster bioinformatic platform at IT Center for Science Finland (https://chipster.csc.fi). All sequences were quality-checked by FASTQC. Sequences were then aligned to Human Sapiens genome GRCh38.95 with TopHat2, assembled with Cufflinks and analyzed for differential gene expression using Cuffdiff. For the latter, differences in FPKM (Fragment Per Kilobase Million) values were considered significant when p-values were equal or less than 0.05. Finally, to predict for possible molecular functional and gene-pathway interactions, the significant differentially expressed genes were queried for over-represented pathways in the ConsensusPathDB-human database (Max Planck Institute, http://cpdb.molgen.mpg.de), which integrates interaction networks from 32 public databases, and the results assessed for statistical significance using hypergeometric distribution probability test.

Work 4 ("*Selenium Compounds Exert Tumor-specific Cytotoxicity on Pancreatic Cancer and Suppress DDR2 and CEMIP in Human Organotypic Cultures*") was a prospective preclinical experimental study. PDAC tumor samples from 9 chemonaïve patients operated at Karolinska University Hospital were cultured for 72 h at atmospheric (21 %) O_2 tension

according to the method previously established in Work 2, except for the addition of diphenyl diselenide. At 24 h, tissue slices were exposed during subsequent 48 h of culture by replacing the culture medium with fresh medium spiked with the following drugs at various concentrations: sodium selenite (Se) at 5 µM, 15 µM and 30 µM; methylselenocysteine (MSC) at 100 µM, 250 µM and 500 µM (single agent) and in combination with 200 µM indole-3-pyruvic acid (IPA); and gemcitabine 1 µM and IPA 200 µM alone. Cultured but untreated slices were used as controls ('Control 72 h'). The different treatment conditions were tested in duplicate slices. When removed from culture, slices were fixed in formalin, embedded in paraffin, and processed for histology. H&E sections were evaluated to confirm the presence of PDAC and to assess the grade of differentiation. Immunohistochemistry for CK19 was performed on all slices from one culture with extensive infiltrate of a poorly differentiated carcinoma to demarcate the tumor regions for subsequent digital image analysis. All histological slides were digitalized at 20X magnification. Histomorphological assessments were performed on whole slide images using QuPath (version 0.2), based on manual annotations or for one culture digital image analysis.

As our previous work 3 revealed during culture the progressive outgrowth of cancer cells along the surface of the tissue slices, this rather than the total tumor content (within the slice) was primarily assessed. The cancer cell outgrowth was manually annotated on H&E-stained digital slide images (n = 109), using different labels for the various cell morphologies: flat/attenuated, cubic, cylindrical, clear, swollen and necro-apoptotic. These were finally simplified and combined into two morphological categories: "viable" (comprising flat, cubic, cylindrical, and clear) and (severely) "damaged" (comprising swollen and necro-apoptotic). These two categories were used for downstream statistical analyses and for the morphological assessment within the slice of two tumors that did not show outgrowth, corresponding to a poorly differentiated carcinoma with solid growth pattern and a moderately differentiated carcinoma with dispersed mode of invasion between pancreatic lobuli in a background of chronic pancreatitis.

Based on the morphological assessments described above, the following readouts were considered as most reliable for the evaluation of drug response in the tissue slices: the percentages of "viable" and "damaged" tumor, the length of cancer cell outgrowth as percentage of the total slice perimeter, and a custom metric, termed tumor viability index, defined as the sum of products of the outgrowth lengths and viability weights, according to the formula "$\Sigma_{i=\text{viable, damaged}}(\%\ \text{outgrowth length}_i * \text{weight}_i)$", where weight = 3 for "viable" and = 1 for "damaged" cancerous outgrowth, respectively.

Quantitative data derived from the annotations were averaged over duplicate slices and processed using R (version 3.6.3). As Shapiro's tests indicated non-normally distributed values, non-parametric Wilcoxon tests were used for matched comparison between cultured but untreated control slices and the different treatment conditions, with Benjamini & Hochberg correction for multiple testing. An adjusted p-value < 0.05 was considered statistically significant.

Transcriptomic analysis was performed for seven cultures with similar methods as described above in Work 3 and for the following conditions: IPA 200 µM, Gemcitabine 1 µM, Se 15 µM, MSC 100 µM, and MSC 100 + IPA 200 µM. Briefly, total RNA was

extracted from formalin-fixed paraffin-embedded sections and used to prepare cDNA libraries. After depletion of ribosomal cDNA, libraries were sequenced using NextSeq. 500 Illumina system, which generated a median of 25 million raw paired-end reads per sample. Processing of sequencing data and differential gene expression analysis using DESeq2 Bioconductor package were performed through Chipster bioinformatic interface at IT Center for Science Finland. Differences in gene expression with adjusted p-value ≤ 0.05 and log2fold change of +1 or -1 were initially considered statistically significant. To identify the most significant differentially expressed genes, results were subsequently filtered using a cut-off p-value of 0.000,1. Heatmaps and dendrograms of RNA expression profiles were generated with Chipster, and volcano plots using the open-source Galaxy platform for computational research (https://galaxyproject.org).

Ethical considerations:

The research in Work 1 was approved by the Regional Ethical Review Board, Stockholm, with diary number 2015/259-31/2. Signed consent from patients was not required due to the retrospective nature of the study and the commonly poor prognosis of the analyzed tumor types.

The research in Works 2-4 was approved by the Regional Ethical Review Board, Stockholm, diary number 2012/1657-31/4. All patients who participated in the studies received oral and written information and they voluntarily signed the consent form regarding inclusion, tissue sampling, culturing, analysis, and collection of associated clinicopathological data. Approval for sample collection (Bbk number 1039) was obtained from Stockholms Medicinska Biobank. In February 2019, an amendment was approved by Etikprövningsmyndigheten (diary number 2019-00788) that gave permission to use the patient's (autologous) serum to further improve culture conditions, to include preoperatively treated (downstaged) PDAC and all types of periampullary cancer (including neuroendocrine tumors) as well as to send tissue samples for analysis in laboratories abroad after signing of a Material Transfer Agreement. In this amendment, an updated patient information sheet compliant with EU's GDPR regulation was also included.

Participation in the studies did not entail any risks to the participant patients, because all investigations were performed exclusively on a small amount of surplus tumor tissue that was neither required for diagnostics nor any other medical care-related purposes. Participation in the study did not entail any possible complications for the participant patients.

There was no direct benefit for the individual patient from taking part in this research. The overall results of the studies may, however, contribute to improve treatment of patients with pancreatic cancer in the future, for example by selecting more effective drugs with the ex-vivo tissue slice culture system.

The risk of damage of personal integrity for participant patients was minimized by pseudonymizing all data and storing the key on a locked computer at the Department of Clinical Pathology and Cytology at Karolinska University Hospital, Huddinge.

Being able to test ex-vivo the individual patient's tumor with different candidate drugs is highly relevant as it has the potential to contribute to the implementation of precision

medicine in clinical practice, by providing guidance for the postoperative treatment. These consequences should be considered beneficial to the patients.

5 RESULTS

Work 1 ("*Immunohistochemical Typing of Adenocarcinomas of the Pancreatobiliary System Improves Diagnosis and Prognostic Stratification*"):

After data pre-processing (analysis of missing data, removal of tumor samples with a high amount of missing data and imputation of missing data in the remaining), the final series for analysis comprised 264 core needle biopsies and 145 resection specimens of ampullary carcinoma (n = 24), pancreatic ductal adenocarcinoma (PDAC; n = 139), distal bile duct cancer (n = 7), gallbladder cancer (n = 37), perihilar cholangiocarcinoma (n = 27), intrahepatic cholangiocarcinoma (n = 97), and hepatocellular carcinoma (n = 78).

Principal component analysis showed no clustering of pancreatobiliary tumors according to the immunohistochemical marker panel or the type of probe (biopsy/resection), disregarding these as potential confounding factors. Unsupervised hierarchical cluster analysis identified four main tumor groups: extrahepatic pancreatobiliary, intestinal, intrahepatic cholangiocarcinoma, and hepatocellular carcinoma. The intestinal group (n = 24) included 8 PDACs, 7 ampullary carcinomas and 4 gallbladder cancers, while 27 intrahepatic cholangiocarcinomas clustered in the extrahepatic pancreatobiliary group. Most PDACs (116 out of 139) clustered in the extrahepatic pancreatobiliary group. The main tumor clusters were further confirmed by using a different clustering technique based on complex network (Figure 5).

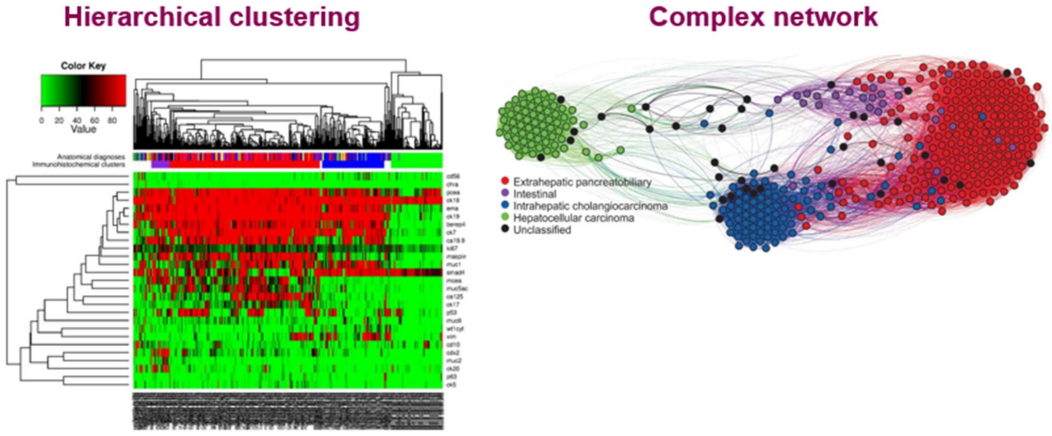

Figure 5 - Clustering of adenocarcinomas of the pancreatobiliary system according to immunohistochemical expression data. Adapted from Fernández Moro C et al. Immunohistochemical Typing of Adenocarcinomas of the Pancreatobiliary System Improves Diagnosis and Prognostic Stratification. PloS One. 2016;11:e0166067. Copyright © 2016 Fernández Moro C et al. CC-BY.

Differential expression analysis revealed the markers with significantly different expression between the various groups (from hierarchical clustering): extrahepatic pancreatobiliary vs intestinal, extrahepatic pancreatobiliary vs intrahepatic cholangiocarcinoma, and intrahepatic

cholangiocarcinoma vs hepatocellular carcinoma. Comparative immunohistograms were generated to visualize differences in expression between the immunohistochemical tumor groups, for the markers that were selected by differential expression analysis, using a cutpoint of 10 % for the extent of positive staining in tumor cells (Figure 6). Complex network visualizations effectively depicted the expression levels of each marker for every individual tumor in the immunohistochemical clusters. These were internally validated by a different approach using machine learning models. Robustness of discrimination between the immunohistochemical tumor groups was confirmed for the full set of (n = 27) markers (average ROC area value about 0.96) and using only the significant markers according to differential expression (average ROC area value 0.95). A simplified immunohistochemical panel of eight makers (CK19, CK20, MUC2, MUC5AC, CA19-9, monoclonal CEA, CA125 and SMAD4) was finally proposed as a guide for the diagnosis of the immunohistochemical tumor types.

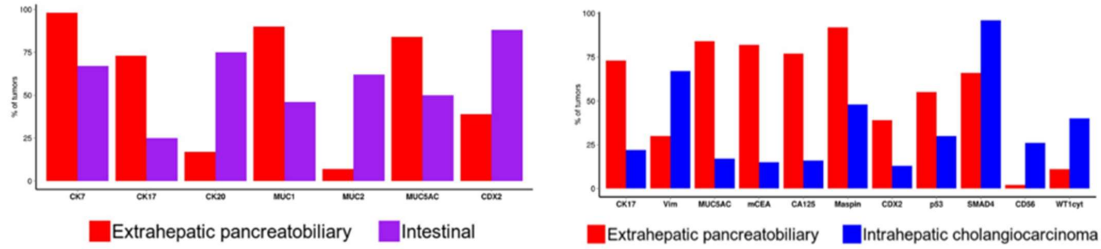

Figure 6 – Comparative immunohistograms depicting the distinguishing markers between the immunohistochemical tumor groups. Adapted from Fernández Moro C et al. Immunohistochemical Typing of Adenocarcinomas of the Pancreatobiliary System Improves Diagnosis and Prognostic Stratification. PloS One. 2016;11:e0166067. Copyright © 2016 Fernández Moro C et al. CC-BY.

Survival analysis was performed for 86 patients who had undergone surgical resection of the primary tumor. The general short overall survival (OS) of non-resected patients (only diagnostic biopsy, median OS = 6 months) precluded a meaningful survival analysis in this group. In the resected group, median OS was 24 months for the extrahepatic pancreatobiliary, 54 months for the intestinal, and 109 months for the intrahepatic cholangiocarcinoma immunohistochemical types. Overall, Cox proportional hazards models including the immunohistochemical tumor classification were statistically significant both in univariate ($p < 0.001$) and multivariate ($p = 0.001$) analyses. In particular, the intestinal type ($p = 0.014$, adjusted HR = 0.19, 95 % CI = 0.05 ± 0.72), pT4 ($p = 0.002$), and pN0 ($p = 0.045$) were independent predictors of OS. In contrast, Cox proportional hazards models including the anatomically-based tumor classification were statistically significant on multivariate analysis ($p = 0.005$), but only pT4 ($p = 0.035$) and pN0 ($p = 0.020$), and not the anatomical tumor location, were independent predictors of OS. When restricting the analysis to the extrahepatic pancreatobiliary and intestinal immunohistochemical types, the latter was consistently associated with a more favorable OS (univariate: $p = 0.025$, crude HR = 0.33, 95 % CI = 0.12–0.91; multivariate: $p = 0.014$, adjusted HR = 0.19; 95 % CI = 0.05–0.71) (Figure 7).

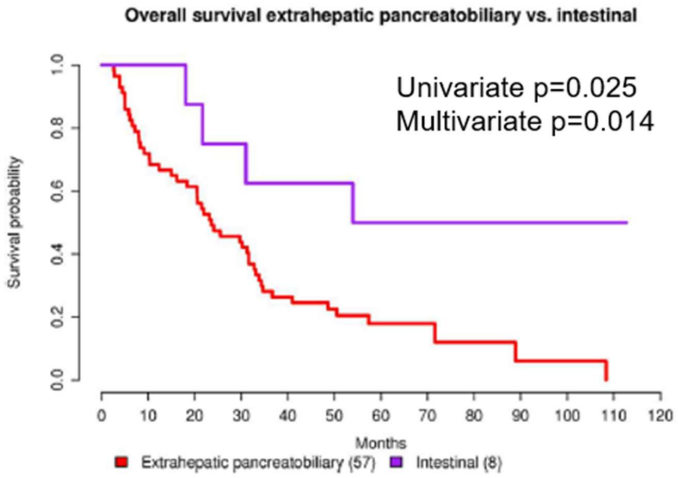

Figure 7 - Kaplan-Meier plot for overall survival by immunohistochemical tumor types. Adapted from Fernández Moro C et al. Immunohistochemical Typing of Adenocarcinomas of the Pancreatobiliary System Improves Diagnosis and Prognostic Stratification. PloS One. 2016;11:e0166067. Copyright © 2016 Fernández Moro C et al. CC-BY.

Work 2 ("*Ex-Vivo Organotypic Culture System of Precision-Cut Slices of Human Pancreatic Ductal Adenocarcinoma*"):

The procedure yielded a median of 14 (range: 12-17) tissue slices, 350 µm in thickness per tumor sample. The median area of tissue slices was 31.9 mm^2 (range: 20.1–57.9 mm^2).

Light microscopic evaluation revealed overall good morphological preservation of the tissue slices during the entire culture period. Necrotic and apoptotic cell death were observed in discrete areas within the first 24 h of culture, while no further tissue damage was observed during subsequent 72 h (Figure 8). Spatial distribution of non-viable tissue areas showed that these were highest in the peripheral zone of the tissue slices, followed by the intermediate one.

Examination by transmission electron microscopy showed that at 72 h, overall, most cell populations, including the cancer cells and cancer associated fibroblasts, maintained ultrastructural integrity. Damage was mainly limited to the endothelial cells and the presence of focal cellular necrosis in cancer cells.

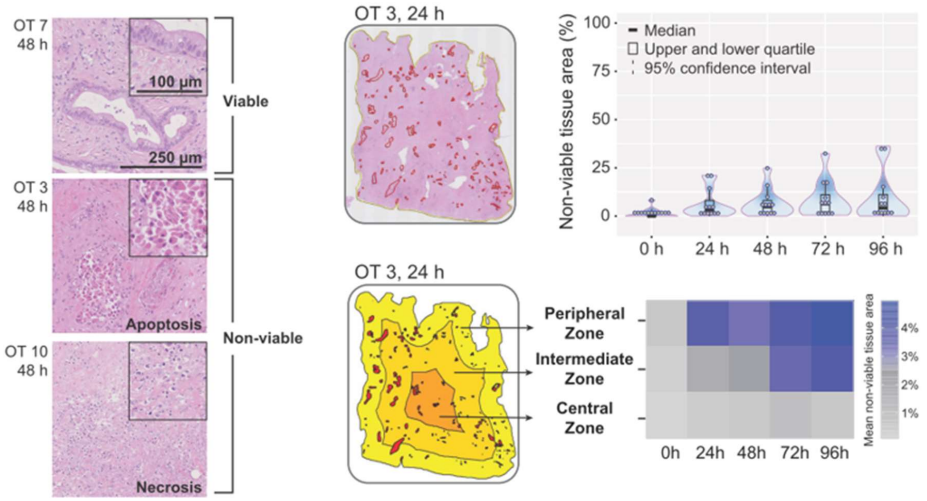

Figure 8 – Analysis of tissue viability in precision-cut PDAC slices. Red annotation areas in central panels indicate non-viable tissue. Photomicrographs, H&E staining. Adapted from Misra S et al. Ex vivo organotypic culture system of precision-cut slices of human pancreatic ductal adenocarcinoma. Sci Rep. 2019 Feb 14;9:2133. Copyright © 2019, Misra S et al. CC-BY.

Each of the cultured adenocarcinomas retained its characteristic histological and cytological features and grade of differentiation (well, moderate to poor, poor non-gland forming) throughout the culture period (0-96 h) (Figure 9).

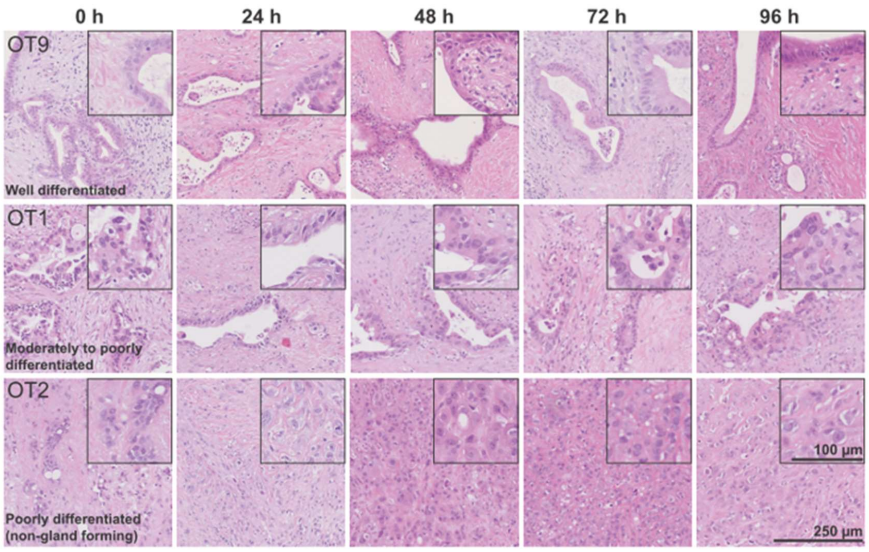

Figure 9 - Tumor histomorphology and grade of differentiation in the tissue slices. H&E staining. From Misra S et al. Ex vivo organotypic culture system of precision-cut slices of

human pancreatic ductal adenocarcinoma. Sci Rep. 2019 Feb 14;9:2133. Copyright © 2019, Misra S et al. CC-BY.

Histological examination revealed during culture the gradual outgrowth of cancer cells and non-neoplastic cells on the surface of the tissue slices (Figure 10). The cancerous cell outgrowth was composed of atypical cells. While the non-neoplastic cell outgrowth consisted mainly of cells that were fairly flat at the beginning of the culture but became progressively taller and cylindrical towards the end, an observation that indicated cellular maturation. Both the cancerous and non-neoplastic cell outgrowths were positive for CK19 and negative for vimentin and trypsin, confirming that these were cancer cells and ductal epithelial cells, respectively. The cancerous phenotype was confirmed by P53 overexpression or SMAD4 negativity. Quantitation data showed that the cancerous cell outgrowth was more extensive than the non-neoplastic one. All together, these findings suggest the involvement of active tissue repair and proliferation in the cultured tissue slices.

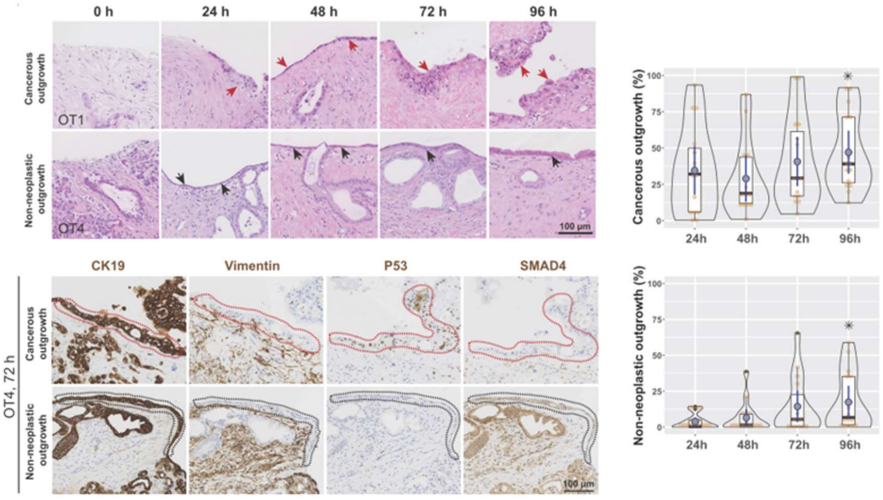

Figure 10 - Cancerous (red arrows and areas) and non-neoplastic (black arrows and areas) cell outgrowths. Top left: H&E staining. Bottom left: immunohistochemistry. Adapted from Misra S et al. Ex vivo organotypic culture system of precision-cut slices of human pancreatic ductal adenocarcinoma. Sci Rep. 2019 Feb 14;9:2133. Copyright © 2019, Misra S et al. CC-BY.

Moreover, cancer cell outgrowth maintained the characteristic cytomorphological features related to the grade of differentiation of the tumor within the tissue slices (Figure 11). Well differentiated tumors formed single-layered outgrowths composed of cells with mildly atypical, polarized nuclei. Moderately differentiated tumors formed outgrowths that showed a variable degree of (pseudo)stratification and were composed of overtly atypical cells with nuclear pleomorphism and loss of polarization. Non-gland forming, poorly differentiated carcinomas developed patchy outgrowths of highly atypical cells that focally tended to detach from the slice surface. Quantitatively, the extent of the cell outgrowth relative to the perimeter of the tissue slice increased with better differentiation grade. At 96 h, the median percentage of the slice perimeter covered by cancer cell outgrowth was 71.2 % (range 20.0–

81.9 %) in well differentiated tumors, 43.9 % (range 39.6–90 %) in moderate to poorly differentiated ones, and 27.3 % (range 12.3–39.0 %) in non-gland forming, poorly differentiated carcinomas.

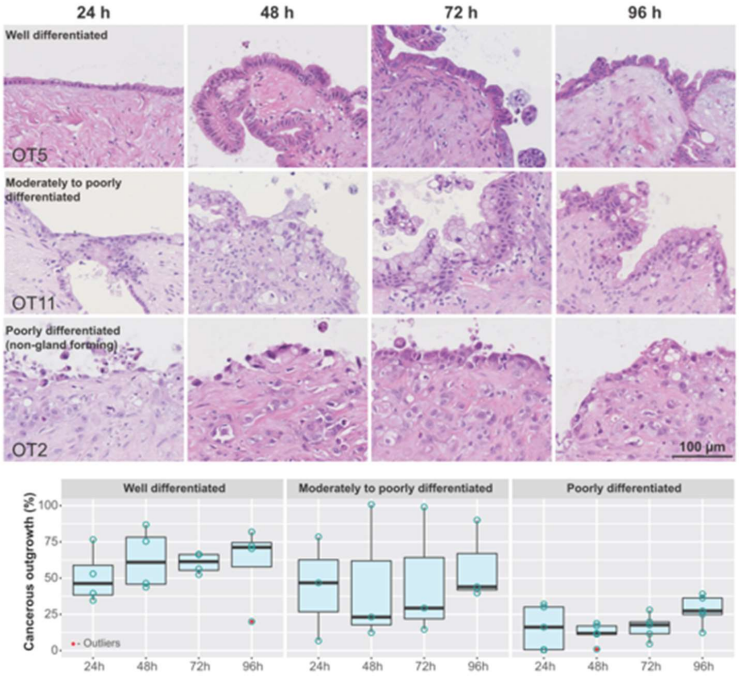

Figure 11 - Cancerous cell outgrowth and grade of tumor differentiation. Top: H&E staining. From Misra S et al. Ex vivo organotypic culture system of precision-cut slices of human pancreatic ductal adenocarcinoma. Sci Rep. 2019 Feb 14;9:2133. Copyright © 2019, Misra S et al. CC-BY.

Although not quantified, it was noticed that in better differentiated tumors the total tumor cell content tended to decrease gradually within the slice during culture time, while it became prominent (as outgrowth) on the slice surface.

The cancer cells continued proliferating (as assessed by Ki67 index) during culture, both within the slice and on the surface (Figure 12). Overall, proliferation was higher within the slice and in poorly differentiated tumors. Over time, proliferation remained steady in poorly differentiated tumors, but tended to decrease in better differentiated ones.

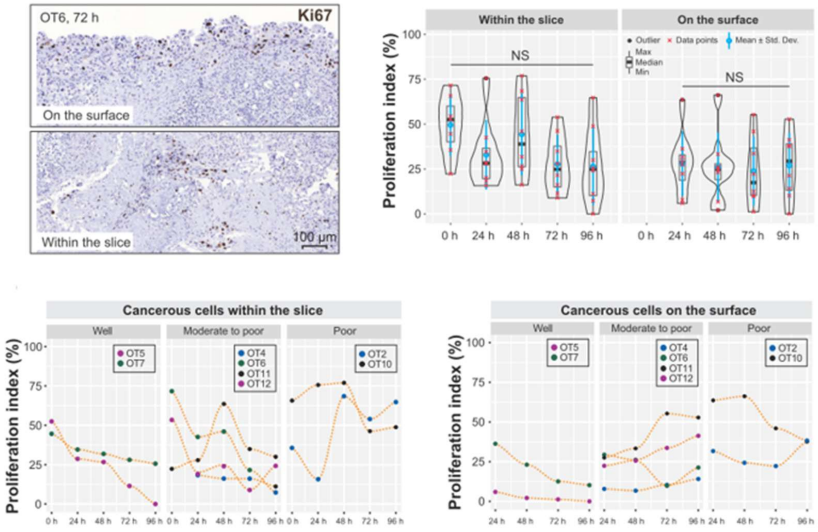

Figure 12 - Cancer cell proliferation. From Misra S et al. Ex vivo organotypic culture system of precision-cut slices of human pancreatic ductal adenocarcinoma. Sci Rep. 2019 Feb 14;9:2133. Copyright © 2019, Misra S et al. CC-BY.

As the mTOR pathway is a central regulator of cellular metabolism and growth, phosphorylation of ribosomal protein S6, downstream of mTOR, was used as a marker of metabolic activity in the tissue slices. The cancer and stroma cells were positive for pS6. The average levels of pS6 in the cancer cells were higher at 24 h when compared to the control, non-cultured slices, and remained stable at later time points.

Following successful preservation of tissue viability under hyperoxic condition (41 % O_2 level), we investigated slice culturing at atmospheric condition, 21 % O_2 level. Morphological analyses did not reveal quantitative differences in tissue viability, cell outgrowth, proliferation, or metabolic activity between paired tissue slices cultured under hyperoxic or atmospheric conditions (Figure 13).

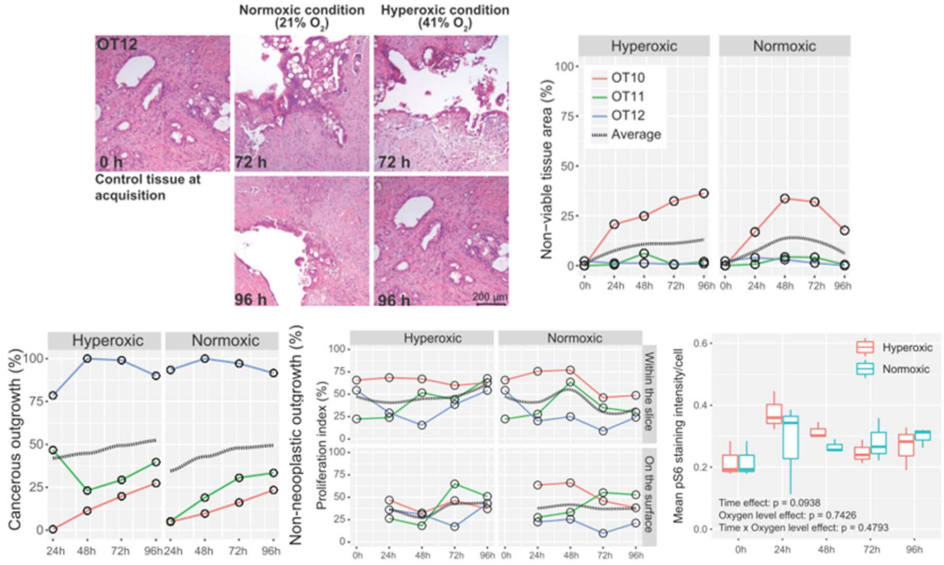

Figure 13 - Tissue viability, cell outgrowth, proliferation and metabolic activity of matched tissue slices cultured under hyperoxic (41 % O_2) and atmospheric (21 % O_2) conditions. Top-left, H&E staining. Adapted from Misra S et al. Ex vivo organotypic culture system of precision-cut slices of human pancreatic ductal adenocarcinoma. Sci Rep. 2019 Feb 14;9:2133. Copyright © 2019, Misra S et al. CC-BY.

As the stroma is a key component of the microenvironment, both the cancer-associated and the residual pancreatic stroma were characterized by immunohistochemistry at 0 and 72 h (Figure 14). At both time points, cancer-associated stroma was positive for vimentin, α-SMA and D2-40, while it was negative for CD34. In contrast, residual pancreatic stroma was positive for vimentin, CD34, and partially for α-SMA, while D2-40 was negative or minimal. Similarly, $CD3^+$ T-cells and $CD68^+$ macrophages were preserved during culture.

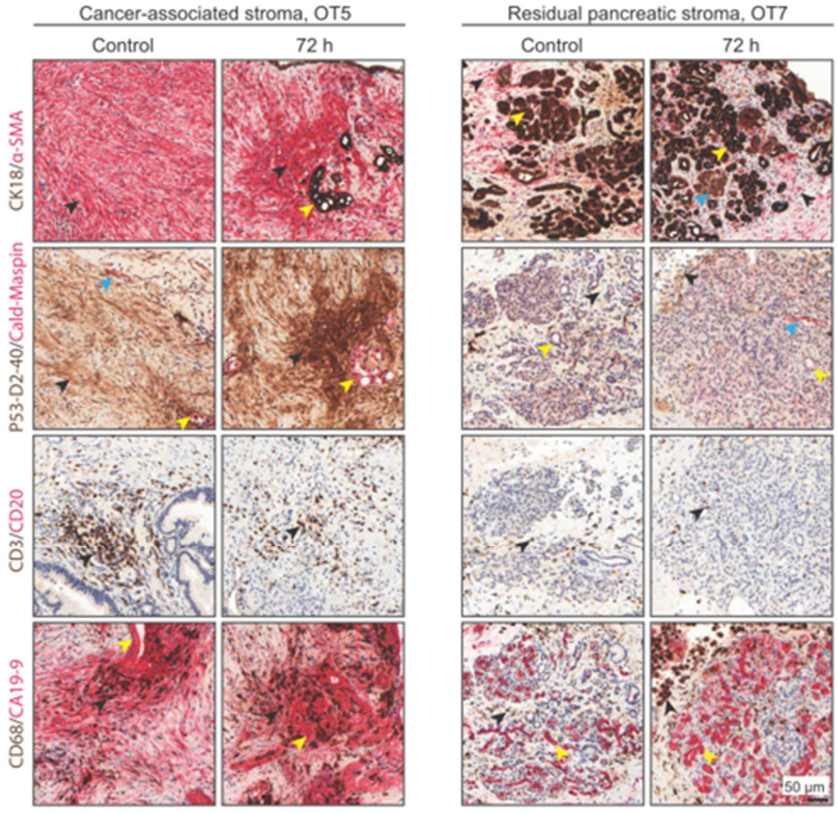

Figure 14 - Immunohistochemical characterization of stroma and immune cells in cultured tissue slices. In cancer-associated stroma: black arrows - cancer associated fibroblasts (α-SMA, D2-40) and immune cells (CD3, CD68), yellow arrows - cancer cells, blue arrow – smooth muscle cells. In residual pancreatic stroma: yellow arrows – pancreatic acini and ducts, blue arrows – islet of Langerhans (CK18) and smooth muscle cells (Cald), black arrows – lobular stroma (α-SMA, D2-40) and immune cells (CD3, CD68). From Misra S et al. Ex vivo organotypic culture system of precision-cut slices of human pancreatic ductal adenocarcinoma. Sci Rep. 2019 Feb 14;9:2133. Copyright © 2019, Misra S et al. CC-BY.

Work 3 ("*Genome-wide Transcriptome Profiling of Ex-Vivo Precision-Cut Slices from Human Pancreatic Ductal Adenocarcinoma*"):

On histomorphology, four out of five analyzed cultures showed, based on data from Work 2, minimal (range 0-6 %) and one mild to moderate (0-18 %) tissue damage, between 0 h (baseline, non-cultured) and 72 h of culture (Figure 15).

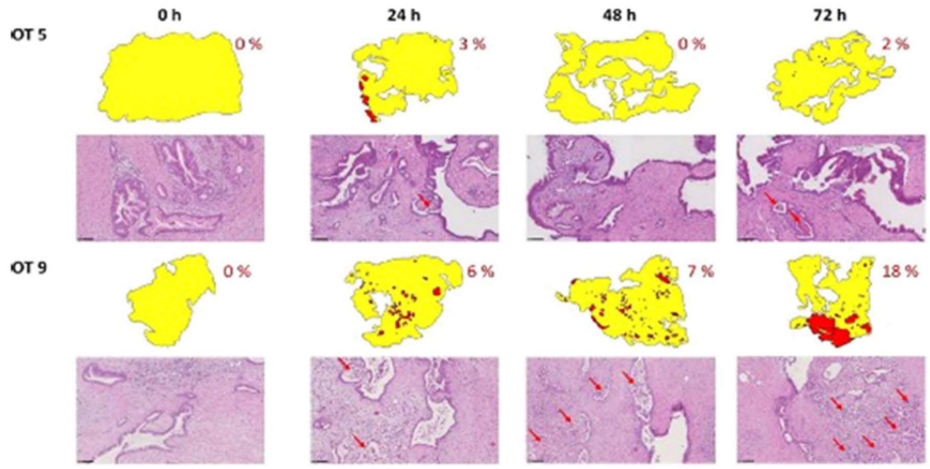

Figure 15 - Morphological viability in representative tissue slice cultures. Red areas (slice diagrams) and arrows (photomicrographs, H&E staining) indicate non-viable tissue regions. Adapted from Ghaderi M et al. Genome-wide Transcriptome Profiling of Ex-Vivo Precision-Cut Slices from Human Pancreatic Ductal Adenocarcinoma. Scientific Reports. 2020 Jun 3;10:9070. Copyright © 2020, Ghaderi M et al. CC-BY.

A total of 58,713 genes (coding and non-coding) and 206,487 gene transcripts were analyzed for differences in expression levels between 24 h intervals (24-72 h) and baseline (0 h). Only a limited number of genes were significantly upregulated (median of 12, 10 and 15 genes) or downregulated (median of 15, 12 and 25 genes) during culture (at 24, 48 and 72 h, respectively), as compared to baseline. No statistically significant differences in transcript isoform expression were detected at any time point.

The list of suggested top three pathways that were significantly overrepresented for each culture, the three time points together (24-72 h), is shown below (Table 1). Cathepsin L (CTSL) was upregulated in all cultures, which together with varying up- or downregulation of matrix metalloproteinase, collagen and laminin transcripts suggested remodeling of the extracellular matrix.

One culture (OT9) with morphologically increased areas of tissue damage showed upregulation of PTGS2, IGFBP1, PMAIP1 and VEGFA genes, which suggests activation of apoptosis via HIF-1/quercetin/NF-κB/AP-1 interaction pathways (138–141). In this culture, several mitochondrial transcripts were also downregulated at 72 h, suggesting a drop in oxidative phosphorylation by downregulation of NADH dehydrogenase (MT-ND1-6) and electron transport chain (MT-CO1-2 and -CYB) activity.

Table 1 - Top 3 significantly suggested pathways (all time points together, 24-72 h) for every culture. From Ghaderi M et al. Genome-wide Transcriptome Profiling of Ex-Vivo Precision-Cut Slices from Human Pancreatic Ductal Adenocarcinoma. Scientific Reports. 2020 Jun 3;10:9070. Copyright © 2020, Ghaderi M et al. CC-BY.

		p-value	Pathway	Database	Mapped genes
OT1	24 h	0.000122	IL-17 signaling pathway - Homo sapiens (human)	KEGG	MAPK10; MUC5AC; CXCL8
	24 h	0.000182	Overview of nanoparticle effects	Wikipathways	CXCL8; CRP
	24 h	0.000431	nfkb activation by nontypeable hemophilus influenzae	BioCarta	CXCL8; MUC5AC
	48 h	0.000724	Collagen degradation	Reactome	MMP14; CTSL
	48 h	0.000784	Innate Immune System	Reactome	CRP; CTSL; TXNIP; OLFM4; SERPINA1; MUC5AC
	48 h	0.00154	Xenobiotics metabolism	EHMN	CYP3A5; AKR1C1
	72 h	0.000724	Collagen degradation	Reactome	MMP14; CTSL
	72 h	0.00392	Phenytoin (Antiarrhythmic) Action Pathway	SMPDB	HYOU1; TNNT2
	72 h	0.00548	Innate Immune System	Reactome	CRP; CTSL; TXNIP; OLFM4; MUC5AC
OT5	24 h	1.12e-05	Validated targets of C-MYC transcriptional repression	PID	HMGCS2; NDRG1; NDRG2; SFRP1
	24 h	0.000266	HIF-1-alpha transcription factor network	PID	ADM; PLIN2; NDRG1
	24 h	0.000877	Sympathetic Nerve Pathway (Neuroeffector Junction)	PharmGKB	ADM; ADRA2C
	48 h	1.92e-05	Inflammatory Response Pathway	Wikipathways	IGHA2; THBS1; IGHM
	48 h	0.0028	Cocaine addiction - Homo sapiens (human)	KEGG	PPP1R1B; CREB3L3
	48 h	0.00326	Peptide hormone metabolism	Reactome	INHBB; SLC30A8
	72 h	0.00153	Sympathetic Nerve Pathway (Neuroeffector Junction)	PharmGKB	ADM; ADRA2C
	72 h	0.00235	Degradation of the extracellular matrix	Reactome	MMP11; CAPN13; CTSL
	72 h	0.0026	Plasma lipoprotein remodeling	Reactome	CREB3L3; ALB
OT9	24 h	3.07e-06	Photodynamic therapy-induced HIF-1 survival signaling	Wikipathways	PTGS2; IGFBP1; PMAIP1; VEGFA
	24 h	7.54e-06	Interleukin-4 and Interleukin-13 signaling	Wikipathways	PTGS2; OSM; VEGFA; F13A1; LIF
	24 h	3.54e-05	HIF-1-alpha transcription factor network	PID	PLIN2; IGFBP1; HK2; VEGFA
	48 h	4.31e-05	Photodynamic therapy-induced HIF-1 survival signaling	Wikipathways	PTGS2; PMAIP1; VEGFA
	48 h	0.000368	Quercetin and Nf-kB- AP-1 Induced Cell Apoptosis	Wikipathways	PTGS2; VEGFA
	48 h	0.000661	S1P1 pathway	PID	PTGS2; VEGFA
	72 h	2.37e-11	Respiratory electron transport	Reactome	MT-CO2; MT-CO1; MT-CYB; …
	72 h	3.11e-11	Electron Transport Chain (OXPHOS system in mitochondria)	Wikipathways	MT-ND6; MT-ND5; MT-ND4;…
	72 h	1.56e-10	Respiratory electron transport, ATP synthesis by chemiosmotic coupling	Reactome	MT-CO2; MT-CO1; MT-CYB; …
OT11	48 h	2.48e-05	AP-1 transcription factor network	PID	FOS; DUSP1; EGR1; PLAU
	48 h	8.59e-05	Pancreatic secretion - Homo sapiens (human)	KEGG	AMY2A; PNLIP; CPA1; CPA2
	48 h	0.000126	ErbB1 downstream signaling	PID	FOS; ZFP36; EGR1; DUSP1
	72 h	1.33e-05	Post-translational protein phosphorylation	Reactome	SPARCL1; CP; F5; SERPINA1; IGFBP1
	72 h	2.69e-05	Regulation of Insulin-like Growth Factor (IGF) transport and uptake by Insulin-like Growth Factor Binding Proteins (IGFBPs)	Reactome	SPARCL1; CP; F5; SERPINA1; IGFBP1
	72 h	0.000316	IL6-mediated signaling events	PID	CRP; FOS; A2M
OT12	24 h	4.01e-06	Collagen formation	Reactome	LAMC2; COL7A1; CTSL; COL21A1
	24 h	2.56e-05	Assembly of collagen fibrils and other multimeric structures	Reactome	LAMC2; CTSL; COL7A1
	24 h	2.97e-05	Anchoring fibril formation	Reactome	COL7A1; LAMC2
	72 h	0.000147	Collagen degradation	Reactome	MMP14; CTSL
	72 h	0.00132	Degradation of the extracellular matrix	Reactome	MMP14; CTSL
	72 h	0.0065	VEGFA-VEGFR2 Signaling Pathway	Wikipathways	MMP14; TXNIP

Work 4 ("*Selenium Compounds Exert Tumor-specific Cytotoxicity on Pancreatic Cancer and Suppress DDR2 and CEMIP in Human Organotypic Cultures*"):

The case series comprised five moderately, two moderately to poorly, and two poorly differentiated carcinomas. Seven out of nine tumors showed a prominent cancer cell outgrowth during culture. This presented several distinct histomorphological appearances ('flat'/attenuated, 'cubic', 'cylindrical') as well as varying degrees of morphological changes that are associated with cellular stress and damage ('clear' > 'swollen' > 'necro-apoptotic') (Figure 16). As described above in Methods, the former ('flat', 'cubic', 'cylindrical' and 'clear'), which were most abundant in untreated slices, were combined as 'viable' for downstream analysis; while the latter ('swollen' and 'necro-apoptotic'), which were most prominent in treated slices, were grouped as 'damaged'. The other two tumors that did not present cell outgrowth were assessed within the slice according to the two-tiered classification.

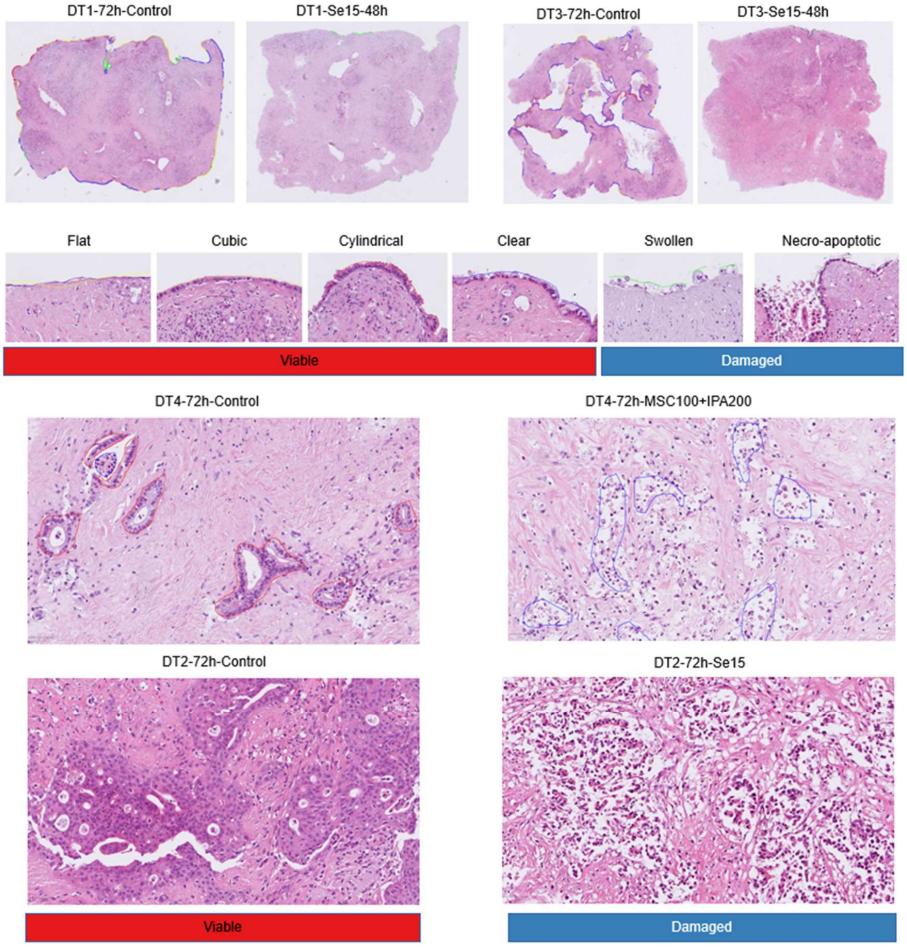

Figure 16 – Representative photomicrographs illustrating the varying morphological appearances of the cancer cells (top) as outgrowth and (bottom) within the slice, H&E staining.

Median overall percentages of tumor (cancer) cell viability, all concentrations together, were 82 %, 9 %, 39 % and 47 % in control, Se and MSC alone or in combination with IPA, respectively. Major tumor responses, defined as a percentage of 'damaged' cancer cells > 90 %, closely corresponding to Evans' (142) tumor regression grades III-IV, were observed for several treatment conditions: Se 30 µM (in n = 7 cultures), Se 15 µM (n = 5), MSC 100 µM, MSC 250-500 µM ± IPA 200 µM (n = 3 each) and MSC 100 µM + IPA 200 µM (n = 2) (Figure 17).

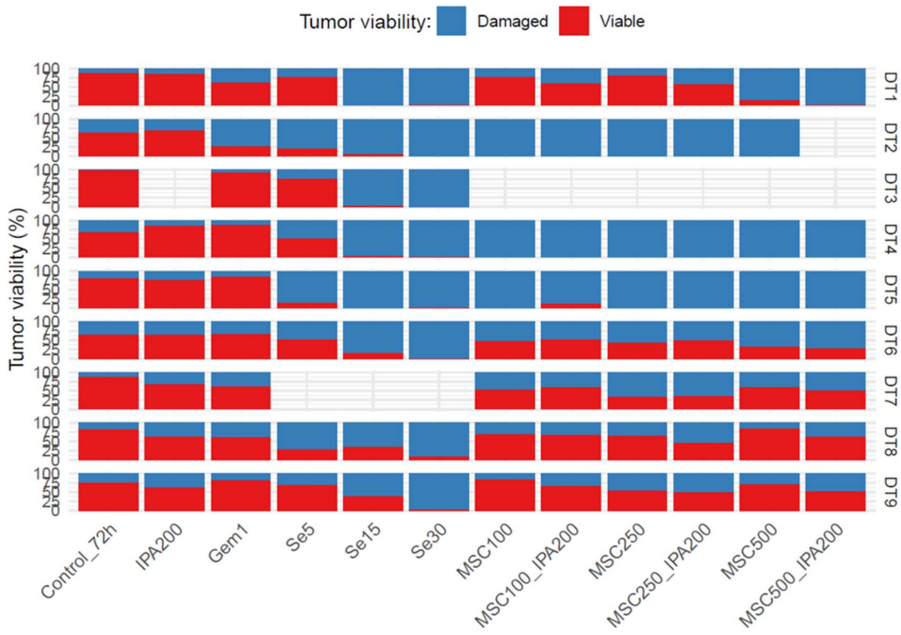

Figure 17 - Tumor viability for every culture and treatment condition.

Se 5-30 µM and MSC 100-500 µM ± IPA 200 µM treatments showed significant reductions in tumor cell viability as compared to matched untreated slices (Control 72 h) (Figure 18). The adjusted p-values ranged between 0.014 and 0.019 and effect sizes between 0.84 and 0.89 (large). Median tumor cell viability ranged from 52.4 % to 1.9 % for Se 5-30 µM, from 52.3 % to 25.1 % for MSC 100-500 µM and from 56.5 % to 30.2 % for MSC 100-500 µM + IPA 200 µM. These values are consistent with a dose-dependent effect of selenium treatment.

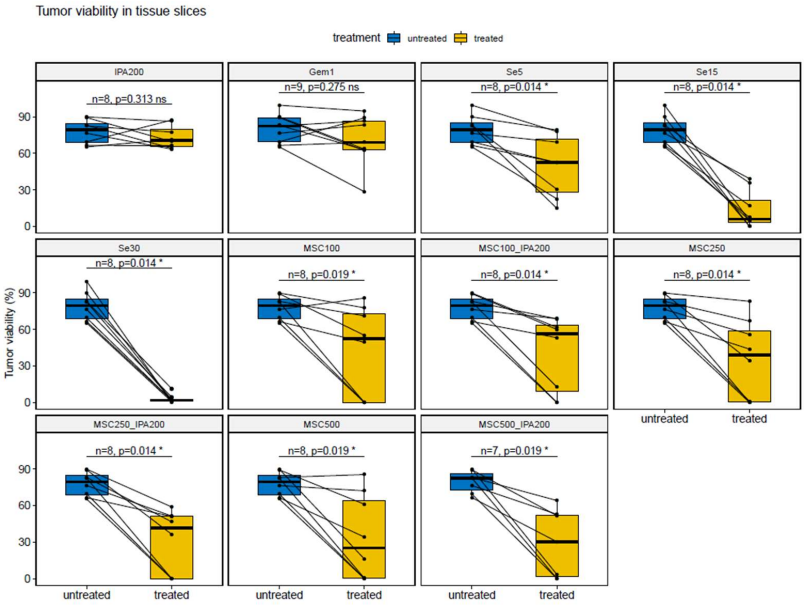

Figure 18 - Differences in tumor viability as compared to untreated controls for every condition.

Median percentages of cancerous outgrowth length, all concentrations together, were 56 %, 24 %, 60 % and 42 % for control, Se and MSC alone or in combination with IPA, respectively. These showed a decreasing trend with selenium treatments as compared to controls, but the differences did not reach statistical significance (Figure 19).

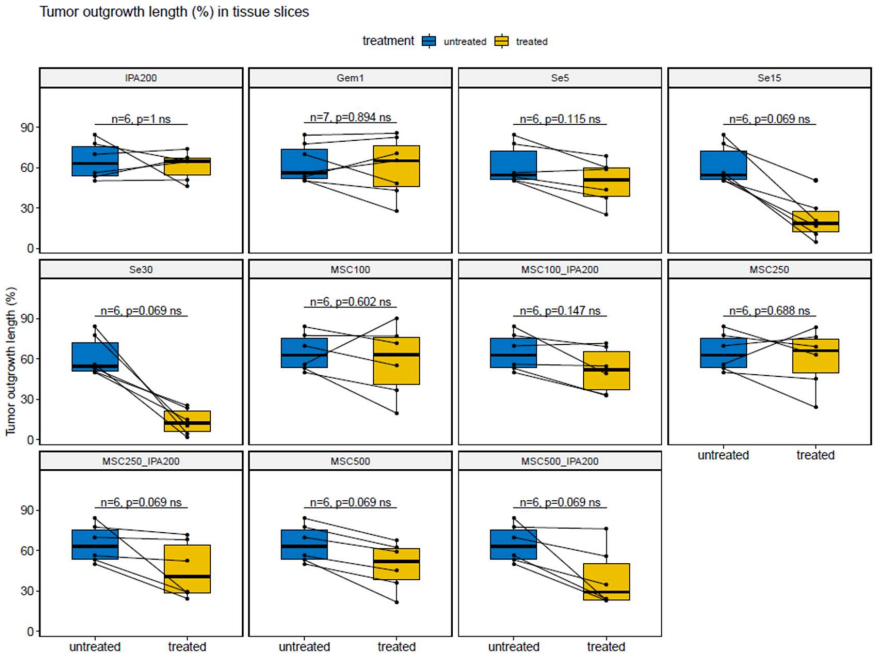

Figure 19 - Differences in cancerous outgrowth length as compared to untreated controls for every condition.

Median values of tumor viability index (sum of products of the outgrowth lengths and viability weights), all concentrations together, were 157, 31, 122, and 96 in control, Se and MSC alone or in combination with IPA, respectively.

Se 5-30 µM, MSC 500 µM and MSC 100-500 µM + IPA 200 µM treatments showed significant reductions in tumor viability index (Figure 20). Adjusted p-values were 0.049 and effect sizes 0.90 (large) each. Median tumor viability index ranged from 117.9 to 14.4 for Se 5-30 µM and from 119.4 to 50.1 for MSC 100-500 µM + IPA 200 µM, consistent with a dose-dependent effect.

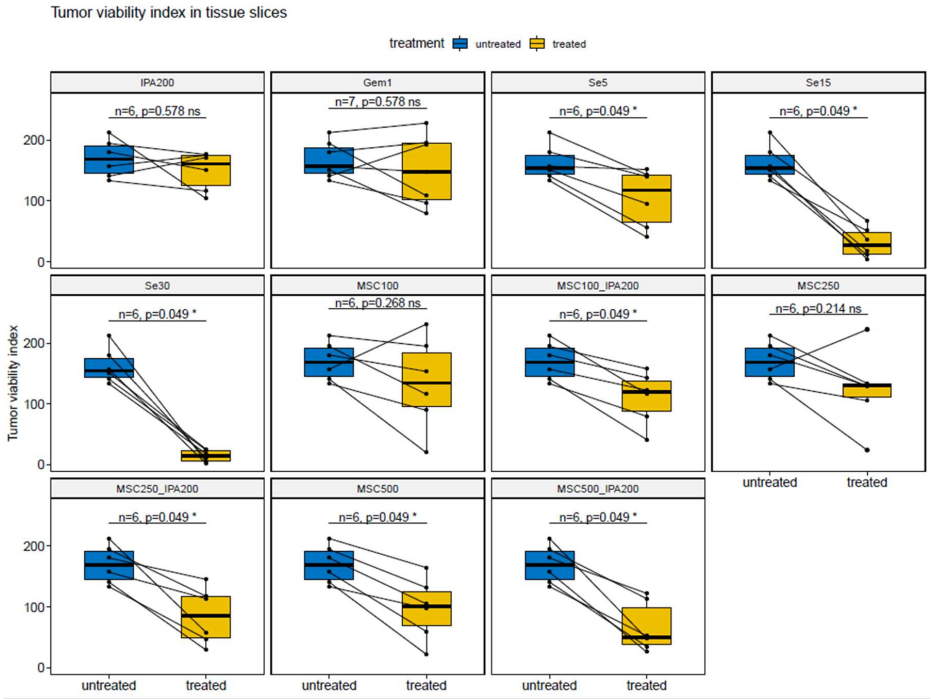

Figure 20 - Differences in tumor viability index as compared to untreated controls for every condition.

Visual histomorphological assessment showed no overt signs of treatment-related damage of the tissue slice stroma (Figure 21).

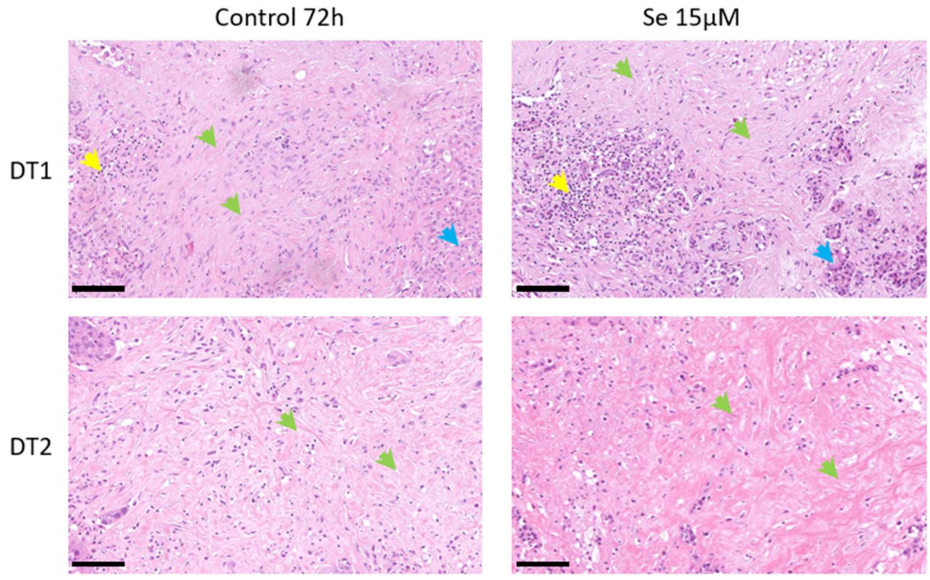

Figure 21 - Representative photomicrographs of the stroma in the tissue slices, H&E staining. Green arrows: preserved stroma. Blue arrows: remnants of pancreatic parenchyma. Yellow arrows: immune cells. Scale bar: 100 µm.

Transcriptomic analysis of Se 15 µM as compared to (untreated) control slices showed upregulation of 1099 (2.1 %) and downregulation of 738 (1.4 %) out of 53594 gene transcripts. Subsequent filtering by a p-value cutpoint of 0.000,1 resulted in a list of 38 highly differentially expressed genes. Specifically, *CEMIP*, *PLOD2*, *DDR2* and *P4HA1*, genes involved in extracellular matrix remodeling, cancer growth and metastatic potential, were significantly downregulated, while the cell death-inducing genes *ATF3* and *ACHE* were significantly upregulated in Se 15 µM treated slices (Figure 22). The top three and most significant associated pathways were the 'Attenuation phase of the heat shock transcriptional response', 'Collagen formation', and 'Heat shock factor 1 (HSF1)-dependent transactivation'. MSC 100 µM treated slices showed significant upregulation of *CRYAB* and *HSB8*, which were likely to be involved in 'HSF1-dependent cellular response upon stress activation' pathway.

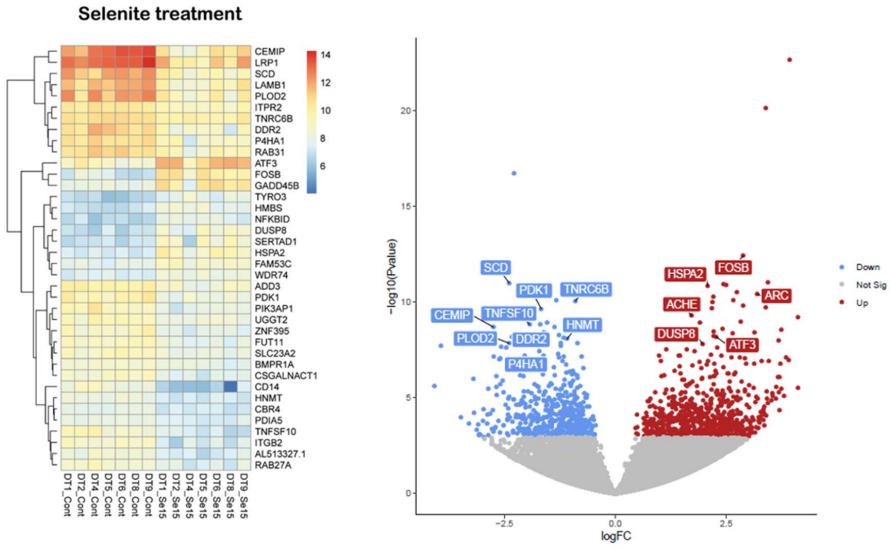

Figure 22 – Heatmap and volcano plot of highly differentially expressed genes between Se 15 µM treatments and untreated controls, p-values < 0.000,1.

6 DISCUSSION

Work 1 ("*Immunohistochemical Typing of Adenocarcinomas of the Pancreatobiliary System Improves Diagnosis and Prognostic Stratification*") developed an immunohistochemical classification that integrated and simplified the anatomy-based (WHO) (137) classification of adenocarcinomas of the pancreatobiliary system: pancreatic ductal adenocarcinoma, ampullary carcinoma, distal bile duct cancer, gallbladder cancer, perihilar cholangiocarcinoma, and intrahepatic cholangiocarcinoma. It introduced three main immunohistochemical types - extrahepatic pancreatobiliary, intestinal, and intrahepatic cholangiocarcinoma - along with their respective characteristic and discriminant markers and showed that the intestinal type was associated with a significantly better survival than the pancreatobiliary type, both in univariate analysis and after adjusting for tumor stage (pT) and lymph node status (pN).

This work contributes further evidence to a number of studies (87,88) that emphasize the histological type (pancreatobiliary vs intestinal) rather than anatomical localization as a determinant factor for overall survival after surgical resection of the primary tumor. In the present series, 8 out of 139 PDAC (6 %) were classified as intestinal type, a slightly lower proportion than reported in previous studies, e.g. Albores-Saavedra et al. 11 out of 110 (10 %) (83) and Bronsert et al. 11 out of 126 (9 %) (88). In previous studies, the pancreatobiliary and intestinal tumor types were categorized mostly based on H&E staining (83), and it was recognized that a fraction of tumors are difficult to classify due to mixed or intermediate histological features (84,88). Similarly, intrahepatic cholangiocarcinoma can be very difficult to distinguish on H&E staining from metastatic adenocarcinoma. Still, 36 out of the 409 tumors in the study cohort could not be meaningfully classified by the unsupervised clustering approach, which is a limitation of the study and may indicate different or intermediate immunohistochemical subtypes. The comprehensive immunohistochemical panels and discriminant markers presented in the study may prove useful to improving the differential diagnosis of pancreatobiliary vs intestinal and intrahepatic cholangiocarcinoma tumor types.

Work 2 ("*Ex-Vivo Organotypic Culture System of Precision-Cut Slices of Human Pancreatic Ductal Adenocarcinoma*") presents a model that is unique in allowing culturing of entire pancreatic cancer tissue, i.e., the cancer cells and their native microenvironment, with good preservation of tissue viability and structural integrity during at least 96 h. Importantly, the cancer cells retain their grade of differentiation and morphological phenotypes, and continue proliferating, while the stroma remains intact. Cancer cells form a progressively extending outgrowth on the surface of the tissue slices, a phenomenon reminiscent of "wound healing". Results were comparable when culturing under hyperoxic (41 % O_2) and atmospheric (21 % O_2) conditions, suggesting that tissue oxygenation was not a limiting factor.

The conventional set-up for drug testing and experimental cancer biology relies significantly on the use of cell lines and genetically engineered or xenograft-based animal models. Even if

these models recapitulate some of the features of human pancreatic cancer, there are important limitations, mainly the lack of the native tumor microenvironment and the use of hosts from different species that may be immunocompromised. For decades, tissue slice cultures have been used to study physiology, metabolism, and toxicity (96). More recently, precision-cut tissue slices have been employed to investigate drug effects in various tumor types, such as breast cancer (100,109), glioblastoma (101,110), and lung cancer (114). When it comes to the pancreas, most previous research has focused on acinar and neuroendocrine cell physiology (105), transfection efficiency for viral-vector-mediated gene therapy (103), pancreatic stellate cell activation (104), and PDAC immunotherapy (108). Some limitations of the slice models are that they are not currently adapted for high-throughput analysis and long-term (weeks to months) culture and that interslice variation makes quantitation and comparison of readouts difficult. The presented model, being a close surrogate of the parent tumor, represents a significant step forward in the search for models that are clinically relevant with a view to precision medicine and tumor biology investigations, as it factors in the tumor microenvironment, in particular the cancer stroma and the immune cell populations.

In **Work 3** ("*Genome-wide Transcriptome Profiling of Ex-Vivo Precision-Cut Slices from Human Pancreatic Ductal Adenocarcinoma*") five tissue slice cultures from Work 2 were characterized at the transcriptome level. Differential expression and pathway overrepresentation analysis revealed that, overall, only a limited number of genes were significantly up- or downregulated at 24 h intervals (24 to 72 h) as compared to baseline (0 h, non-cultured). One culture with increased areas of tissue damage on histomorphological assessment showed upregulation of VEGFA and PTGS2, a finding that highly likely reflects activation of HIF-1-triggered cell apoptosis.

Davies et al. (102) performed thorough characterizations of precision-cut tissue slices from different human and animal model derived tumors and found that hypoxia and stress of the tissue slices were associated with HIF-1α overexpression on immunohistochemistry. In the present work, VEGFA and HIF-1 pathways were upregulated specifically in a culture with increased tissue damage, which is in line with the observation by Davies et al. A limitation of the study is that bulk transcriptomic analysis was performed for the entire slice tissue, while microdissection was not performed to enrich specifically for tumor content. The study results support that transcriptomic analysis is a valuable complement to morphology for the evaluation of precision-cut tissue slice cultures.

In **Work 4** ("*Selenium Compounds Exert Tumor-specific Cytotoxicity on Pancreatic Cancer and Suppress DDR2 and CEMIP in Human Organotypic Cultures*") the previously established tissue slice model (in Works 2 and 3) was used to investigate cytotoxic effects in human PDAC using a panel of two selenium compounds (selenite and methylselenocystein) at various concentrations. Morphology based quantitations showed pronounced decreases in tumor viability after 48 h of exposure to Se at doses of 15 µM and 30 µM. These were associated at the transcriptome level by upregulation of the cell death-inducing genes ATF3

(143) and ACHE (144), and downregulation of CEMIP (hyaluronan degradation) (145), PLOD2 (146), DDR2 (147) and P4HA1 (148), genes involved in extracellular matrix remodeling, cancer growth and metastatic potential.

During the past decade, a growing number of studies have used ex-vivo slice cultures to address key questions related to oncogenic signaling pathways (97), intratumoral heterogeneity (114), drug responses (109,112), and oncoimmunology (108,110). The present study further supports that tissue slice cultures are a suitable model for drug sensitivity testing in samples of surgically resected human PDAC.

The marked responses to Se 15-30 μM observed in the present study are in line with the cytotoxic effects reported in previous experiments in cell lines. Moreover, the doses in the range 15-30 μM are below the maximum tolerated dose of selenium in humans, as previously reported in a phase I clinical trial by our group (136).

The study has some limitations. Further readouts associated with response to treatment such as total tumor cell content, apoptotic/cell death fraction and functional assays of tumor cell viability, which may be suitable for the assessment of cancer types that form large, compact masses, could not be applied due to the intrinsic features of PDAC: the presence of a prominent stroma, a lower tumor cell density, and a more disperse tumor growth, commonly intermixed with remnants of non-neoplastic pancreatic parenchyma. Time-lapse from drug exposure to slice harvesting may also impact the possibility of read-out detection, e.g., apoptotic markers (M30, activated caspase 3) could no longer be detected in preliminary experiments in a fraction of severely damaged/necrotic cancer cells, likely due to protein degradation at advanced phases of cell death. The reasons above led us conclude that a thorough assessment of cancer cell morphology was the most reliable and consistent readout for evaluation of drug response-associated cell damage in precision-cut tissue slices of human PDAC after selenium treatment. Finally, bulk RNA analysis, i.e., with inclusion of the tumor microenvironment, was performed.

7 CONCLUSIONS

Work 1 ("*Immunohistochemical Typing of Adenocarcinomas of the Pancreatobiliary System Improves Diagnosis and Prognostic Stratification*"):

Integrative immunohistochemical classification of adenocarcinomas of the pancreatobiliary system revealed three main immunohistochemical types: extrahepatic pancreatobiliary, intestinal, and intrahepatic cholangiocarcinoma and their characteristic and discriminant markers.

Independent of anatomic location, the prognostically more favorable intestinal type can be distinguished from the more aggressive pancreatobiliary type.

The characteristic immunohistochemical profile of intrahepatic cholangiocarcinoma positively supports its pathological diagnosis, which is commonly regarded as a diagnosis of exclusion (of metastatic adenocarcinoma).

Work 2 ("*Ex-Vivo Organotypic Culture System of Precision-Cut Slices of Human Pancreatic Ductal Adenocarcinoma*"):

Ex-vivo culture of precision-cut tissue slices enables the preservation of pancreatic cancer tissue in its entirety for at least 96 h and cancer cells retain their grade of differentiation, proliferation, and metabolic activity. The tumor microenvironment is preserved, including cancer-associated stroma and immune cell populations.

Cultures of precision-cut PDAC slices provide a close approximation of the in-situ tumor in the patient. As such, they may constitute an unparalleled, short-term, high-content model for drug sensitivity testing and for the analysis of the complex interactions between cancer cells and their microenvironment.

Work 3 ("*Genome-wide Transcriptome Profiling of Ex-Vivo Precision-Cut Slices from Human Pancreatic Ductal Adenocarcinoma*"):

Genome-wide transcriptome analysis supports that ex-vivo cultured tissue slices of PDAC may be a representative model of the tumor tissue in-vivo, also at the molecular level.

Transcriptome analysis was found to be a valuable complement to morphology for the evaluation of ex-vivo cultured tissue slices.

Work 4 ("*Selenium Compounds Exert Tumor-specific Cytotoxicity on Pancreatic Cancer and Suppress DDR2 and CEMIP in Human Organotypic Cultures*"):

Redox-active selenium compounds are promising candidate chemotherapeutic agents for the treatment of PDAC. The most pronounced effects were observed by selenite (Se) in a dose-dependent manner.

This ex-vivo model is relatively inexpensive, gives results within days and helps reducing animal experiments.

Precision-cut tissue slice cultures of tumor samples from surgical specimens are a novel, promising tool for drug sensitivity testing. They enable a wide range of applications spanning from drug discovery to personalized cancer medicine in which a panel of drugs may be tested on the cognate, patient-derived malignant tumor.

8 POINTS OF PERSPECTIVE

Pancreatic cancer is currently the 4th leading cause of cancer-related death in the West. As it is projected to rank 2nd by 2030, it can be regarded a medical emergency. Despite advances in surgery and modest survival improvements with current chemotherapies, a breakthrough that dramatically improves survival is still awaited.

PDAC is currently recognized as a (histomorphologically, immunohistochemically, and molecularly) heterogeneous disease, and therapeutically actionable subtypes are beginning to emerge. It is foreseeable that novel subtypes and classification schemes will be unveiled in the ongoing quest for precision and personalized medicine for patients with PDAC (149). It is conceivable that patients with tumors of the less aggressive intestinal type may benefit from tailored oncological treatment, e.g., more in line with colorectal cancer, and the possibility of resection of liver metastases. Future clinical trials would benefit from stratifying patients according to established PDAC subtypes.

Tissue slice models may constitute a state-of-the-art tool for drug sensitivity testing and the implementation of personalized cancer medicine. To fully unfold their potential for oncology and tumor biology applications, further optimizations would be valuable, such as:

- Improvements in tissue viability to consistently render the entire slice volume available for morphological and molecular assessments, investigations of tumor-microenvironment interactions and experimental manipulations (anticancer drugs, pathway inhibitors and agonists).
- Increase culture time with comparable viability, to enable experimental manipulations and assessment of temporal effects in the order of 7-10 days.
- Establish an array of robust, correlated readouts at multiple levels (morphology-based labellings, genome/transcriptome/proteome, functional assays on the supernatants) to systematically assess the tissue slices.
- Develop tailored digital image analysis pipelines for the automated and unbiased quantitation of labelled targets in the cancerous, stromal and immune cell populations and for the assessment of the spatial relations between them.
- Machine learning/AI techniques may prove useful to analyze and integrate the multidimensional readouts and provide meaningful and clinically relevant results based on previous slice culture analyses and their connection with clinical response and outcome data.

The marked cytostatic effects observed in ex-vivo cultured precision-cut tissue slices of human PDAC treated with selenium compounds highlight these as promising candidate drugs for the treatment of this still devastating disease. The results merit further investigations, including animal experiments and clinical trials.

The intensively pursued therapeutic breakthrough that significantly curbs PDAC progression will benefit many patients, also opening the possibility of surgery for patients currently deemed to be non-operable due to locally advanced or metastatic disease.

9 ACKNOWLEDGEMENTS

I would like to express my most sincere gratitude to my supervisors, co-authors, collaborators, colleagues, friends, and to my family. For your inestimable and continuous support during these years of building this thesis. I would need a hundred pages to name you all, so I will have to restrain myself, but know that I am deeply grateful for all you have done and that it has been a great honor to be and share knowledge, work, and experiences with all of you!

Caroline Sophie Verbeke, my main supervisor. Thank you for bringing me to the research path and for your always wise, patient, and gentle guidance and advice. Thank you for expanding my mind with innumerable, most enriching discussions, and for your extraordinary contributions and support to pancreatic cancer research and pancreas pathology. Wish you all happiness and success in the beautiful neighboring country!

Mikael Björnstedt, my co-supervisor. Thank you for your constant support and trust. Thank you for your enthusiasm, driving energy, wise direction and for building a great, multidisciplinary pancreatic and liver research team. Thank you for empowering research and innovation and for bringing them close to the clinical bench. Wish you all the best and greatest success!

Matthias Löhr, my co-supervisor. Thank you for your kind and constant support and your enlightening mentorship. Thank you for believing in the value of this thesis' works since inception and your invaluable contributions to making it happen. Thank you for always being there and help. Wish you all the best and greatest success in all your projects!

Béla Bozóky, my Maestro in pathology. Thank you for your gentle and continuous support and mentorship in the path of pathology. Thank you for teaching us your fellow pathologists and residents to look better, deeper and for pointing to the most difficult cells and asking us "What is this?". Thank you for your passion towards knowledge and research, for your humble wisdom, for the countless evenings looking slides together and for teaching me the art of immunohistochemistry. You are the soul of the clinic and our dear Maestro!

Soledad Pouso Elduayen, my Uruguayan mother 😉 in Sweden and master of this thesis' pivotal histology operations. Thank you for your continuous help and tireless work to obtain the best tissue slices and stainings. Thank you for taking such a good care of everyone in the research group, of me in rough times of medical stances and for showing me how to take care of orchids!

Mehran Ghaderi, our molecular pathology expert. Thank you for expanding the minds of us morphologists with amazing insights from your thorough transcriptome analyses. Thank you for developing molecular pathology in the clinic and being always in search for actionable gene fusions!

Joakim Dillner, thank you for supporting these works and for greatly enhancing our understanding of their underlying molecular dimension. Thank you for promoting and empowering research and education in the clinic.

Arun Selvam, my research group colleague. Thank you for your incomparable art in the laboratory, culturing and treating the tissue slices. Thank you for many enlightening group discussions and relevant insights into the cytotoxic mechanisms of selenium compounds. Wish you happiness and greatest success in your career.

Masih Ostad Novin, my collaborator and colleague at the immune lab. No one on Earth can barely match the magic you do with antibodies, automated immunostainers and colorful multiplex immunohistochemical stainings.

Ali Razaghi, my research group colleague. Thank you for many interesting group discussions and for introducing us to the complex world of anticancer cytokines. Wish you happiness and greatest success in your career.

Timea Szekerczes, my research group colleague. Thank you for the relevant group discussions and for expanding the future perspectives of this thesis' work. Wish you happiness and greatest success in your career.

Attila Szakos, my clinic chief. Thank you for your trust and support and for always upholding and promoting research, innovation, and education in the clinic. Thank you for taking such a good care and supporting your coworkers.

Maura Krook, our research nurse. It is thanks to your continuous and inestimable work and engagement that these projects could be developed. My most sincere gratitude.

Marco Gerling, my collaborator. Thank you for your continuous encouragement to pursue research and for your resolution to promote research among our younger fellows. Thank you for so many enlightening discussions on tumor biology and for bringing us the possibility to connect pathology with clinical, experimental, and molecular dimensions.

Benedek Bozóky, my collaborator. Thank you for the fascinating research ideas and discussions, and for your gentle presence and care in rough medical periods.

Helen Kaipe and Laia Gorchs, my collaborators. Thank you for the enlightening discussions and insights into the arcane world of the tumor immune microenvironment. Wish you greatest success in all your research!

Margaret Sällberg Chen, my collaborator. Thank you for your friendly support to pancreas research and for bringing into focus the relevant analyses of pancreatic cystic fluid, its metabolome and microbiome.

Alejandro Fernandez-Woodbridge, my collaborator. You make magic with R and convert raw numbers into amazing and colorful networks where data appear like exotic planets to explore.

Rainer Heuchel, thank you for many inspiring discussions, your invaluable help to set up this thesis project and your tireless work and support to pancreatic research.

Sam Ghazi, my team leader and grand expert in pancreatic pathology. Thank you for your trust and support both in the clinic and research, and for creating such an awesome teamwork environment in the pancreas. Thank you for the enlightening discussions and for always being there to help me solving difficult cases. Wish you all happiness and great success also in your career as writer! We all are "teonauts" in this planet 😉.

Katalin Fekete and **Mátyás Béndek**, my colleagues in the pancreas pathology team. It has always been a great pleasure and honor working with you. Thank you for the enlightening case discussions and your continuous help and support.

Avesta Mahmoud, Dalia Abdulamir, Gunilla Pettersson, Haifa Zablook, Hamide Azizpour, Ida Robertsson, Mats Parnemyr, **Nina Shafiee, Olga Johansson, Pegah Kaviani, Rhadika Adhikari, Selvi Jeyaselvi Kanagarajah and Sofia Murtada** my esteemed lab colleagues in pancreas and biobank. Thank you for your excellent work, your invaluable help, your good spirit in the long afternoons grossing specimens and the wonderful pancreas histology slides you create.

Hans Glaumann, Nikos Papadogiannakis, Olof Danielsson and **Sonia Shtembari**, my maestros and colleagues in liver pathology. Thank you for many enlightening discussions, for your invaluable help in solving difficult cases, and your continuous support to research in the clinic. A great pleasure and honor to learn and work with you.

Laszlo Szekely, my collaborator and colleague. Thank you for enlightening us with your great knowledge and experience in molecular biology. Thank you for being always ready to help and to collaborate in exciting biotechnology endeavors throughout the globe.

Danyil Kuznyecov, my collaborator. Thank you for your engagement and friendly support along these years. Thank you for your enthusiasm and hard work in our attempt to teach AI the art of pathology diagnosis. You are creating the future.

Hicham El Attar, my collaborator. Thank you for your energy and drive bringing the state-of-the-art of pathology diagnosis (digital, molecular) to serve cancer patients in Morocco, my other country, and other African countries. Thank you for connecting professional networks and strengthening the bonds of international collaboration.

Cecilia Strömberg, Christian Sturesson, Ernesto Sparrelid, **Gabriel Saliba**, **Marcus Holmberg, Melroy Alistair D'Souza, Poya Ghorbani**, **Stefan Gilg, Stefan Linder** and all colleagues at the **Upper GI section**. Thank you for your outstanding and tireless work. A great pleasure and honor working with such an excellent pancreatic and liver surgery team!

Francisco Baldaque Silva, Nikolaos Kartalis, Raffaella Poci and all colleagues in Pancreas and Liver Radiology and Endoscopy. Thank you for many enlightening discussions, your outstanding work, and exciting research interactions.

Our former colleagues with whom worked in the clinic and research. **Alexei Terman, Asif Halimi, Elena Rangelova, Jessica Norberg, Marco del Chiaro, Roberto Valente, Sougat Misra, Urban Arnelo, and Xuan Li**. You are indeed missed!

To all present and former colleagues at the **Department of Clinical Pathology and Cytology**. You are top!

To my dear friends **Nacho de la Vega** and **Cristina de Silva**, high-energy active particles of creativity and love. Fiummmmm!

To my dear friends in my hometown (Xixón), **Carlinos, Carolina, César, Edu, Evina, Jessica, Lorena, Luis, Maria, Mayca, Mónica, Natalia, Pablo, Raquelina, Virchi, Xuanin, Xuan Zem**; in Barcelona/Barna, **Alex/Bellini**, **Luis, Marta, Mónica, Rosana, Xavi**; in Amsterdam, **Anke, Filip** and little **Oliver**; and in Essaouira, **Imad/Gnaoui**. For all the wonderful moments together. You know who you are to me. Distance is just an illusion, I bring you in my heart. My dear friends in Sweden, **Ana, Kamal, Salah/Dino, Shekib, and Rolander family**. Thank you for being my family here in Sweden.

Piera Catalano, "cara amica" and wonderful pathologist. I am so thankful to have you in my life. Wish all the best to you and **your wonderful girls**!

Marco Scarpinati, "caro amico", a brother, a father, who encouraged me to start research and do PhD. You had to leave us too early. But "there's no final goodbye, we just say I'll see you down the road". In memoriam.

Eduardo Fuente Martin, thank you for your good advice and for sharing with me your wise lessons from a life dedicated to pathology. I look forward to seeing you in Xixón and enjoying our "café de patólogos".

My family friends, **Ester, Javi, Rocio and Silvia**. Thank you for your love, care, and support since childhood. We are indeed family. And thank you for the delicious Asturias delicatessen, a treasure for us!

To my beloved parents **José Maria Fernández Cordón and Marisa Moro González**. THANK YOU for everything! To my dear **Biba (Sofia El Fakir)** and all my family in Spain, my dear brother **Jorge Fernández Moro** and my sister-in-law **Susana LLamazares**, my grandma **Lola**, my uncle **Jesusín**, my aunt **Inés**, my cousin **Virginia,** and her sweet baby **Minerva**; and all my family in Morocco, **Faida Khallil, Madani El Fakir, Wafa/Wafina El Fakir, Ratiba El Fakir, Anas Fahmi, Khalti Zhor, Ammi Ouzahra, Hbibi Mustapha, Tata Samya, Ammi Hassan, toute la famille Aboulkhatib, tous les cousins, les grands et les adorables petits**. Thank you for your love, patience, embrace, unwavering support, and all the delicious food. All that has come good is due to **You**. A special wink to our dear nephews **Douduo (Adam Hani) the great football player**, **Mael Fernández Llamazares the great athlete**, and all the young ones in the family. Wish you all happiness in life and greatest success in the pursue of your dreams!

10 REFERENCES

1. Barrett K, Barman S, Boitano S, Brooks H. Ganong's Review of Medical Physiology, 23rd Edition. 23 edition. New York: McGraw-Hill Education / Medical; 2009. 726 p.

2. Bray F, Ferlay J, Soerjomataram I, Siegel RL, Torre LA, Jemal A. Global cancer statistics 2018: GLOBOCAN estimates of incidence and mortality worldwide for 36 cancers in 185 countries. CA Cancer J Clin. 2018 Nov;68(6):394–424.

3. Ayoubi S, Johansson E, Toorell N, Bergman O, Fredholm L, Hont G, et al. CANCER I SIFFROR 2018. Socialstyrelsen and Cancerfonden; 2018.

4. Rahib L, Smith BD, Aizenberg R, Rosenzweig AB, Fleshman JM, Matrisian LM. Projecting cancer incidence and deaths to 2030: the unexpected burden of thyroid, liver, and pancreas cancers in the United States. Cancer Res. 2014 Jun 1;74(11):2913–21.

5. Mizrahi JD, Surana R, Valle JW, Shroff RT. Pancreatic cancer. Lancet Lond Engl. 2020 Jun 27;395(10242):2008–20.

6. Basturk O, Hong S-M, Wood LD, Adsay NV, Albores-Saavedra J, Biankin AV, et al. A Revised Classification System and Recommendations From the Baltimore Consensus Meeting for Neoplastic Precursor Lesions in the Pancreas. Am J Surg Pathol. 2015 Dec;39(12):1730–41.

7. Adsay V, Mino-Kenudson M, Furukawa T, Basturk O, Zamboni G, Marchegiani G, et al. Pathologic Evaluation and Reporting of Intraductal Papillary Mucinous Neoplasms of the Pancreas and Other Tumoral Intraepithelial Neoplasms of Pancreatobiliary Tract: Recommendations of Verona Consensus Meeting. Ann Surg. 2016 Jan;263(1):162–77.

8. Hruban RH, Wilentz RE, Kern SE. Genetic progression in the pancreatic ducts. Am J Pathol. 2000 Jun;156(6):1821–5.

9. Molin MD, Matthaei H, Wu J, Blackford A, Debeljak M, Rezaee N, et al. Clinicopathological correlates of activating GNAS mutations in intraductal papillary mucinous neoplasm (IPMN) of the pancreas. Ann Surg Oncol. 2013 Nov;20(12):3802–8.

10. Survival Rates for Pancreatic Cancer [Internet]. [cited 2019 Jun 10]. Available from: https://www.cancer.org/cancer/pancreatic-cancer/detection-diagnosis-staging/survival-rates.html

11. Signs and Symptoms of Pancreatic Cancer [Internet]. [cited 2019 Jun 10]. Available from: https://www.cancer.org/cancer/pancreatic-cancer/detection-diagnosis-staging/signs-and-symptoms.html

12. Pancreatic Cancer - Statistics [Internet]. Cancer.Net. [cited 2019 Jun 10]. Available from: https://www.cancer.net/cancer-types/pancreatic-cancer/statistics

13. Pancreatic Cancer - Types of Treatment [Internet]. Cancer.Net. 2018 [cited 2019 Jun 10]. Available from: https://www.cancer.net/cancer-types/pancreatic-cancer/types-treatment

14. Pancreatic Cancer Prognosis | Pancreatic Cancer Survival, Pancreas Cancer Prognostic [Internet]. Pancreatica. [cited 2019 Jun 10]. Available from: https://pancreatica.org/pancreatic-cancer/pancreatic-cancer-prognosis/

15. Kardosh A, Lichtensztajn DY, Gubens MA, Kunz PL, Fisher GA, Clarke CA. Long-Term Survivors of Pancreatic Cancer: A California Population-Based Study. Pancreas. 2018;47(8):958–66.

16. Oettle H, Post S, Neuhaus P, Gellert K, Langrehr J, Ridwelski K, et al. Adjuvant chemotherapy with gemcitabine vs observation in patients undergoing curative-intent resection of pancreatic cancer: a randomized controlled trial. JAMA. 2007 Jan 17;297(3):267–77.

17. Neoptolemos JP, Stocken DD, Friess H, Bassi C, Dunn JA, Hickey H, et al. A randomized trial of chemoradiotherapy and chemotherapy after resection of pancreatic cancer. N Engl J Med. 2004 Mar 18;350(12):1200–10.

18. Neoptolemos JP, Palmer DH, Ghaneh P, Psarelli EE, Valle JW, Halloran CM, et al. Comparison of adjuvant gemcitabine and capecitabine with gemcitabine monotherapy in patients with resected pancreatic cancer (ESPAC-4): a multicentre, open-label, randomised, phase 3 trial. Lancet Lond Engl. 2017 11;389(10073):1011–24.

19. Janssen QP, Buettner S, Suker M, Beumer BR, Addeo P, Bachellier P, et al. Neoadjuvant FOLFIRINOX in patients with borderline resectable pancreatic cancer: a systematic review and patient-level meta-analysis. J Natl Cancer Inst. 2019 May 14;

20. Conroy T, Hammel P, Hebbar M, Ben Abdelghani M, Wei AC, Raoul J-L, et al. FOLFIRINOX or Gemcitabine as Adjuvant Therapy for Pancreatic Cancer. N Engl J Med. 2018 20;379(25):2395–406.

21. Conroy T, Desseigne F, Ychou M, Bouché O, Guimbaud R, Bécouarn Y, et al. FOLFIRINOX versus gemcitabine for metastatic pancreatic cancer. N Engl J Med. 2011 May 12;364(19):1817–25.

22. Von Hoff DD, Ervin T, Arena FP, Chiorean EG, Infante J, Moore M, et al. Increased survival in pancreatic cancer with nab-paclitaxel plus gemcitabine. N Engl J Med. 2013 Oct 31;369(18):1691–703.

23. Nevala-Plagemann C, Hidalgo M, Garrido-Laguna I. From state-of-the-art treatments to novel therapies for advanced-stage pancreatic cancer. Nat Rev Clin Oncol. 2020 Feb;17(2):108–23.

24. Neesse A, Michl P, Frese KK, Feig C, Cook N, Jacobetz MA, et al. Stromal biology and therapy in pancreatic cancer. Gut. 2011 Jun;60(6):861–8.

25. Buchholz M, Biebl A, Neesse A, Wagner M, Iwamura T, Leder G, et al. SERPINE2 (protease nexin I) promotes extracellular matrix production and local invasion of pancreatic tumors in vivo. Cancer Res. 2003 Aug 15;63(16):4945–51.

26. Lunardi S, Muschel RJ, Brunner TB. The stromal compartments in pancreatic cancer: are there any therapeutic targets? Cancer Lett. 2014 Feb 28;343(2):147–55.

27. Löhr M, Schmidt C, Ringel J, Kluth M, Müller P, Nizze H, et al. Transforming growth factor-beta1 induces desmoplasia in an experimental model of human pancreatic carcinoma. Cancer Res. 2001 Jan 15;61(2):550–5.

28. Thayer SP, di Magliano MP, Heiser PW, Nielsen CM, Roberts DJ, Lauwers GY, et al. Hedgehog is an early and late mediator of pancreatic cancer tumorigenesis. Nature. 2003 Oct 23;425(6960):851–6.

29. Hwang RF, Moore T, Arumugam T, Ramachandran V, Amos KD, Rivera A, et al. Cancer-associated stromal fibroblasts promote pancreatic tumor progression. Cancer Res. 2008 Feb 1;68(3):918–26.

30. Xu Z, Vonlaufen A, Phillips PA, Fiala-Beer E, Zhang X, Yang L, et al. Role of pancreatic stellate cells in pancreatic cancer metastasis. Am J Pathol. 2010 Nov;177(5):2585–96.

31. Hessmann E, Patzak MS, Klein L, Chen N, Kari V, Ramu I, et al. Fibroblast drug scavenging increases intratumoural gemcitabine accumulation in murine pancreas cancer. Gut. 2018;67(3):497–507.

32. Neesse A, Bauer CA, Öhlund D, Lauth M, Buchholz M, Michl P, et al. Stromal biology and therapy in pancreatic cancer: ready for clinical translation? Gut. 2019;68(1):159–71.

33. Catenacci DVT, Junttila MR, Karrison T, Bahary N, Horiba MN, Nattam SR, et al. Randomized Phase Ib/II Study of Gemcitabine Plus Placebo or Vismodegib, a Hedgehog Pathway Inhibitor, in Patients With Metastatic Pancreatic Cancer. J Clin Oncol Off J Am Soc Clin Oncol. 2015 Dec 20;33(36):4284–92.

34. Kim EJ, Sahai V, Abel EV, Griffith KA, Greenson JK, Takebe N, et al. Pilot clinical trial of hedgehog pathway inhibitor GDC-0449 (vismodegib) in combination with gemcitabine in patients with metastatic pancreatic adenocarcinoma. Clin Cancer Res Off J Am Assoc Cancer Res. 2014 Dec 1;20(23):5937–45.

35. Rhim AD, Oberstein PE, Thomas DH, Mirek ET, Palermo CF, Sastra SA, et al. Stromal elements act to restrain, rather than support, pancreatic ductal adenocarcinoma. Cancer Cell. 2014 Jun 16;25(6):735–47.

36. Özdemir BC, Pentcheva-Hoang T, Carstens JL, Zheng X, Wu C-C, Simpson TR, et al. Depletion of carcinoma-associated fibroblasts and fibrosis induces immunosuppression and accelerates pancreas cancer with reduced survival. Cancer Cell. 2014 Jun 16;25(6):719–34.

37. Kunk PR, Bauer TW, Slingluff CL, Rahma OE. From bench to bedside a comprehensive review of pancreatic cancer immunotherapy. J Immunother Cancer. 2016;4:14.

38. Collins MA, Bednar F, Zhang Y, Brisset J-C, Galbán S, Galbán CJ, et al. Oncogenic Kras is required for both the initiation and maintenance of pancreatic cancer in mice. J Clin Invest. 2012 Feb;122(2):639–53.

39. Fukunaga A, Miyamoto M, Cho Y, Murakami S, Kawarada Y, Oshikiri T, et al. CD8+ tumor-infiltrating lymphocytes together with CD4+ tumor-infiltrating lymphocytes and

dendritic cells improve the prognosis of patients with pancreatic adenocarcinoma. Pancreas. 2004 Jan;28(1):e26-31.

40. Protti MP, De Monte L. Immune infiltrates as predictive markers of survival in pancreatic cancer patients. Front Physiol. 2013;4:210.

41. Gorchs L, Fernández Moro C, Bankhead P, Kern KP, Sadeak I, Meng Q, et al. Human Pancreatic Carcinoma-Associated Fibroblasts Promote Expression of Co-inhibitory Markers on CD4+ and CD8+ T-Cells. Front Immunol. 2019;10:847.

42. De Monte L, Reni M, Tassi E, Clavenna D, Papa I, Recalde H, et al. Intratumor T helper type 2 cell infiltrate correlates with cancer-associated fibroblast thymic stromal lymphopoietin production and reduced survival in pancreatic cancer. J Exp Med. 2011 Mar 14;208(3):469–78.

43. Fridman WH, Pagès F, Sautès-Fridman C, Galon J. The immune contexture in human tumours: impact on clinical outcome. Nat Rev Cancer. 2012 15;12(4):298–306.

44. Duan X, Deng L, Chen X, Lu Y, Zhang Q, Zhang K, et al. Clinical significance of the immunostimulatory MHC class I chain-related molecule A and NKG2D receptor on NK cells in pancreatic cancer. Med Oncol Northwood Lond Engl. 2011 Jun;28(2):466–74.

45. Chen W, Wang J, Jia L, Liu J, Tian Y. Attenuation of the programmed cell death-1 pathway increases the M1 polarization of macrophages induced by zymosan. Cell Death Dis. 2016 Feb 25;7:e2115.

46. Ostrand-Rosenberg S, Sinha P. Myeloid-derived suppressor cells: linking inflammation and cancer. J Immunol Baltim Md 1950. 2009 Apr 15;182(8):4499–506.

47. Mace TA, Ameen Z, Collins A, Wojcik S, Mair M, Young GS, et al. Pancreatic cancer-associated stellate cells promote differentiation of myeloid-derived suppressor cells in a STAT3-dependent manner. Cancer Res. 2013 May 15;73(10):3007–18.

48. Roda O, Ortiz-Zapater E, Martínez-Bosch N, Gutiérrez-Gallego R, Vila-Perelló M, Ampurdanés C, et al. Galectin-1 is a novel functional receptor for tissue plasminogen activator in pancreatic cancer. Gastroenterology. 2009 Apr;136(4):1379–90, e1-5.

49. Ene-Obong A, Clear AJ, Watt J, Wang J, Fatah R, Riches JC, et al. Activated pancreatic stellate cells sequester CD8+ T cells to reduce their infiltration of the juxtatumoral compartment of pancreatic ductal adenocarcinoma. Gastroenterology. 2013 Nov;145(5):1121–32.

50. Feig C, Jones JO, Kraman M, Wells RJB, Deonarine A, Chan DS, et al. Targeting CXCL12 from FAP-expressing carcinoma-associated fibroblasts synergizes with anti-PD-L1 immunotherapy in pancreatic cancer. Proc Natl Acad Sci U S A. 2013 Dec 10;110(50):20212–7.

51. Erkan M, Michalski CW, Rieder S, Reiser-Erkan C, Abiatari I, Kolb A, et al. The activated stroma index is a novel and independent prognostic marker in pancreatic ductal adenocarcinoma. Clin Gastroenterol Hepatol Off Clin Pract J Am Gastroenterol Assoc. 2008 Oct;6(10):1155–61.

52. Moffitt RA, Marayati R, Flate EL, Volmar KE, Loeza SGH, Hoadley KA, et al. Virtual microdissection identifies distinct tumor- and stroma-specific subtypes of pancreatic ductal adenocarcinoma. Nat Genet. 2015 Oct;47(10):1168–78.

53. Knudsen ES, Vail P, Balaji U, Ngo H, Botros IW, Makarov V, et al. Stratification of Pancreatic Ductal Adenocarcinoma: Combinatorial Genetic, Stromal, and Immunologic Markers. Clin Cancer Res Off J Am Assoc Cancer Res. 2017 Aug 1;23(15):4429–40.

54. Laklai H, Miroshnikova YA, Pickup MW, Collisson EA, Kim GE, Barrett AS, et al. Genotype tunes pancreatic ductal adenocarcinoma tissue tension to induce matricellular fibrosis and tumor progression. Nat Med. 2016;22(5):497–505.

55. Elyada E, Bolisetty M, Laise P, Flynn WF, Courtois ET, Burkhart RA, et al. Cross-species single-cell analysis of pancreatic ductal adenocarcinoma reveals antigen-presenting cancer-associated fibroblasts. Cancer Discov. 2019 Jan 1;CD-19-0094.

56. Biffi G, Oni TE, Spielman B, Hao Y, Elyada E, Park Y, et al. IL1-Induced JAK/STAT Signaling Is Antagonized by TGFβ to Shape CAF Heterogeneity in Pancreatic Ductal Adenocarcinoma. Cancer Discov. 2019;9(2):282–301.

57. Öhlund D, Handly-Santana A, Biffi G, Elyada E, Almeida AS, Ponz-Sarvise M, et al. Distinct populations of inflammatory fibroblasts and myofibroblasts in pancreatic cancer. J Exp Med. 2017 06;214(3):579–96.

58. Öhlund D, Elyada E, Tuveson D. Fibroblast heterogeneity in the cancer wound. J Exp Med. 2014 Jul 28;211(8):1503–23.

59. Sugimoto H, Mundel TM, Kieran MW, Kalluri R. Identification of fibroblast heterogeneity in the tumor microenvironment. Cancer Biol Ther. 2006 Dec;5(12):1640–6.

60. Kumar V, Boucher Y, Liu H, Ferreira D, Hooker J, Catana C, et al. Noninvasive Assessment of Losartan-Induced Increase in Functional Microvasculature and Drug Delivery in Pancreatic Ductal Adenocarcinoma. Transl Oncol. 2016 Oct;9(5):431–7.

61. Kim S, Toyokawa H, Yamao J, Satoi S, Yanagimoto H, Yamamoto T, et al. Antitumor effect of angiotensin II type 1 receptor blocker losartan for orthotopic rat pancreatic adenocarcinoma. Pancreas. 2014 Aug;43(6):886–90.

62. Liu X, Gündel B, Li X, Liu J, Wright A, Löhr M, et al. 3D heterospecies spheroids of pancreatic stroma and cancer cells demonstrate key phenotypes of pancreatic ductal adenocarcinoma. Transl Oncol. 2021 May 1;14(7):101107.

63. Ikenaga N, Ohuchida K, Mizumoto K, Cui L, Kayashima T, Morimatsu K, et al. CD10+ pancreatic stellate cells enhance the progression of pancreatic cancer. Gastroenterology. 2010 Sep;139(3):1041–51, 1051.e1-8.

64. Lenggenhager D, Amrutkar M, Sántha P, Aasrum M, Löhr J-M, Gladhaug IP, et al. Commonly Used Pancreatic Stellate Cell Cultures Differ Phenotypically and in Their Interactions with Pancreatic Cancer Cells. Cells. 2019 Jan 5;8(1).

65. Verbeke C. Morphological heterogeneity in ductal adenocarcinoma of the pancreas - Does it matter? Pancreatol Off J Int Assoc Pancreatol IAP Al. 2016 Jun;16(3):295–301.

66. Ligorio M, Sil S, Malagon-Lopez J, Nieman LT, Misale S, Di Pilato M, et al. Stromal Microenvironment Shapes the Intratumoral Architecture of Pancreatic Cancer. Cell. 2019 May 23;

67. Sántha P, Lenggenhager D, Finstadsveen A, Dorg L, Tøndel K, Amrutkar M, et al. Morphological Heterogeneity in Pancreatic Cancer Reflects Structural and Functional Divergence. Cancers. 2021 Feb 20;13(4).

68. Gill AJ, Klimstra DS, Lam AK, Washington MK, editors. Tumours of the pancreas. In: WHO Classification of Tumours Digestive system tumours. 5 edition. Lyon: World Health Organization; 2019. p. 295–371.

69. Paal E, Thompson LD, Frommelt RA, Przygodzki RM, Heffess CS. A clinicopathologic and immunohistochemical study of 35 anaplastic carcinomas of the pancreas with a review of the literature. Ann Diagn Pathol. 2001 Jun;5(3):129–40.

70. Kardon DE, Thompson LD, Przygodzki RM, Heffess CS. Adenosquamous carcinoma of the pancreas: a clinicopathologic series of 25 cases. Mod Pathol Off J U S Can Acad Pathol Inc. 2001 May;14(5):443–51.

71. Hameed O, Xu H, Saddeghi S, Maluf H. Hepatoid carcinoma of the pancreas: a case report and literature review of a heterogeneous group of tumors. Am J Surg Pathol. 2007 Jan;31(1):146–52.

72. Wilentz RE, Goggins M, Redston M, Marcus VA, Adsay NV, Sohn TA, et al. Genetic, immunohistochemical, and clinical features of medullary carcinoma of the pancreas: A newly described and characterized entity. Am J Pathol. 2000 May;156(5):1641–51.

73. Deckard-Janatpour K, Teplitz RL, Min BH, Ruebner BH, Gumerlock PH. Undifferentiated carcinoma with osteoclast-like giant cells of the pancreas and periampullary region. Cancer. 1998 Sep 1;83(5):1051–2.

74. Tracey KJ, O'Brien MJ, Williams LF, Klibaner M, George PK, Saravis CA, et al. Signet ring carcinoma of the pancreas, a rare variant with very high CEA values. Immunohistologic comparison with adenocarcinoma. Dig Dis Sci. 1984 Jun;29(6):573–6.

75. Lüttges J, Beyser K, Pust S, Paulus A, Rüschoff J, Klöppel G. Pancreatic mucinous noncystic (colloid) carcinomas and intraductal papillary mucinous carcinomas are usually microsatellite stable. Mod Pathol Off J U S Can Acad Pathol Inc. 2003 Jun;16(6):537–42.

76. Khayyata S, Basturk O, Adsay NV. Invasive micropapillary carcinomas of the ampullo-pancreatobiliary region and their association with tumor-infiltrating neutrophils. Mod Pathol Off J U S Can Acad Pathol Inc. 2005 Nov;18(11):1504–11.

77. Bagci P, Andea AA, Basturk O, Jang K-T, Erbarut I, Adsay V. Large duct type invasive adenocarcinoma of the pancreas with microcystic and papillary patterns: a potential microscopic mimic of non-invasive ductal neoplasia. Mod Pathol Off J U S Can Acad Pathol Inc. 2012 Mar;25(3):439–48.

78. Adsay V, Logani S, Sarkar F, Crissman J, Vaitkevicius V. Foamy gland pattern of pancreatic ductal adenocarcinoma: a deceptively benign-appearing variant. Am J Surg Pathol. 2000 Apr;24(4):493–504.

79. Kim L, Liao J, Zhang M, Talamonti M, Bentrem D, Rao S, et al. Clear cell carcinoma of the pancreas: histopathologic features and a unique biomarker: hepatocyte nuclear factor-1beta. Mod Pathol Off J U S Can Acad Pathol Inc. 2008 Sep;21(9):1075–83.

80. Dursun N, Feng J, Basturk O, Bandyopadhyay S, Cheng JD, Adsay VN. Vacuolated cell pattern of pancreatobiliary adenocarcinoma: a clinicopathological analysis of 24 cases of a poorly recognized distinctive morphologic variant important in the differential diagnosis. Virchows Arch Int J Pathol. 2010 Dec;457(6):643–9.

81. Fagih M, Serra S, Chetty R. Paucicellular infiltrating ductal carcinoma of pancreas: an unusual variant. Ann Diagn Pathol. 2007 Feb;11(1):46–8.

82. Kelly PJ, Shinagare S, Sainani N, Hong X, Ferrone C, Yilmaz O, et al. Cystic papillary pattern in pancreatic ductal adenocarcinoma: a heretofore undescribed morphologic pattern that mimics intraductal papillary mucinous carcinoma. Am J Surg Pathol. 2012 May;36(5):696–701.

83. Albores-Saavedra J, Simpson K, Dancer Y-J, Hruban R. Intestinal type adenocarcinoma: a previously unrecognized histologic variant of ductal carcinoma of the pancreas. Ann Diagn Pathol. 2007 Feb;11(1):3–9.

84. Reid MD, Balci S, Ohike N, Xue Y, Kim GE, Tajiri T, et al. Ampullary carcinoma is often of mixed or hybrid histologic type: an analysis of reproducibility and clinical relevance of classification as pancreatobiliary versus intestinal in 232 cases. Mod Pathol Off J U S Can Acad Pathol Inc. 2016;29(12):1575–85.

85. Fernández Moro C, Fernandez-Woodbridge A, Alistair D'souza M, Zhang Q, Bozoky B, Kandaswamy SV, et al. Immunohistochemical Typing of Adenocarcinomas of the Pancreatobiliary System Improves Diagnosis and Prognostic Stratification. PloS One. 2016;11(11):e0166067.

86. Westgaard A, Schjølberg AR, Cvancarova M, Eide TJ, Clausen OPF, Gladhaug IP. Differentiation markers in pancreatic head adenocarcinomas: MUC1 and MUC4 expression indicates poor prognosis in pancreatobiliary differentiated tumours. Histopathology. 2009 Feb;54(3):337–47.

87. Westgaard A, Tafjord S, Farstad IN, Cvancarova M, Eide TJ, Mathisen O, et al. Pancreatobiliary versus intestinal histologic type of differentiation is an independent prognostic factor in resected periampullary adenocarcinoma. BMC Cancer. 2008 Jun 11;8:170.

88. Bronsert P, Kohler I, Werner M, Makowiec F, Kuesters S, Hoeppner J, et al. Intestinal-type of differentiation predicts favourable overall survival: confirmatory clinicopathological analysis of 198 periampullary adenocarcinomas of pancreatic, biliary, ampullary and duodenal origin. BMC Cancer. 2013 Sep 22;13:428.

89. Chang DK, Jamieson NB, Johns AL, Scarlett CJ, Pajic M, Chou A, et al. Histomolecular phenotypes and outcome in adenocarcinoma of the ampulla of vater. J Clin Oncol Off J Am Soc Clin Oncol. 2013 Apr 1;31(10):1348–56.

90. Collisson EA, Bailey P, Chang DK, Biankin AV. Molecular subtypes of pancreatic cancer. Nat Rev Gastroenterol Hepatol. 2019 Apr;16(4):207–20.

91. Bailey P, Chang DK, Nones K, Johns AL, Patch A-M, Gingras M-C, et al. Genomic analyses identify molecular subtypes of pancreatic cancer. Nature. 2016 Mar 3;531(7592):47–52.

92. Chan-Seng-Yue M, Kim JC, Wilson GW, Ng K, Figueroa EF, O'Kane GM, et al. Transcription phenotypes of pancreatic cancer are driven by genomic events during tumor evolution. Nat Genet. 2020 Feb;52(2):231–40.

93. N Kalimuthu S, Wilson GW, Grant RC, Seto M, O'Kane G, Vajpeyi R, et al. Morphological classification of pancreatic ductal adenocarcinoma that predicts molecular subtypes and correlates with clinical outcome. Gut. 2020 Feb;69(2):317–28.

94. Nicolle R, Blum Y, Duconseil P, Vanbrugghe C, Brandone N, Poizat F, et al. Establishment of a pancreatic adenocarcinoma molecular gradient (PAMG) that predicts the clinical outcome of pancreatic cancer. EBioMedicine. 2020 Jul;57:102858.

95. Tiriac H, Belleau P, Engle DD, Plenker D, Deschênes A, Somerville TDD, et al. Organoid Profiling Identifies Common Responders to Chemotherapy in Pancreatic Cancer. Cancer Discov. 2018 Sep;8(9):1112–29.

96. de Kanter R, Monshouwer M, Meijer DKF, Groothuis GMM. Precision-cut organ slices as a tool to study toxicity and metabolism of xenobiotics with special reference to non-hepatic tissues. Curr Drug Metab. 2002 Feb;3(1):39–59.

97. Vaira V, Fedele G, Pyne S, Fasoli E, Zadra G, Bailey D, et al. Preclinical model of organotypic culture for pharmacodynamic profiling of human tumors. Proc Natl Acad Sci U S A. 2010 May 4;107(18):8352–6.

98. Longati P, Jia X, Eimer J, Wagman A, Witt M-R, Rehnmark S, et al. 3D pancreatic carcinoma spheroids induce a matrix-rich, chemoresistant phenotype offering a better model for drug testing. BMC Cancer. 2013 Feb 27;13:95.

99. Norberg KJ, Liu X, Fernández Moro C, Strell C, Nania S, Blümel M, et al. A novel pancreatic tumour and stellate cell 3D co-culture spheroid model. BMC Cancer. 2020 May 27;20(1):475.

100. Holliday DL, Moss MA, Pollock S, Lane S, Shaaban AM, Millican-Slater R, et al. The practicalities of using tissue slices as preclinical organotypic breast cancer models. J Clin Pathol. 2013 Mar;66(3):253–5.

101. Merz F, Gaunitz F, Dehghani F, Renner C, Meixensberger J, Gutenberg A, et al. Organotypic slice cultures of human glioblastoma reveal different susceptibilities to treatments. Neuro-Oncol. 2013 Jun;15(6):670–81.

102. Davies EJ, Dong M, Gutekunst M, Närhi K, van Zoggel HJAA, Blom S, et al. Capturing complex tumour biology in vitro: histological and molecular characterisation of precision cut slices. Sci Rep. 2015 Dec 9;5:17187.

103. van Geer M-A, Kuhlmann KFD, Bakker CT, ten Kate FJW, Oude Elferink RPJ, Bosma PJ. Ex-vivo evaluation of gene therapy vectors in human pancreatic (cancer) tissue slices. World J Gastroenterol. 2009 Mar 21;15(11):1359–66.

104. Rebours V, Albuquerque M, Sauvanet A, Ruszniewski P, Lévy P, Paradis V, et al. Hypoxia pathways and cellular stress activate pancreatic stellate cells: development of an organotypic culture model of thick slices of normal human pancreas. PloS One. 2013;8(9):e76229.

105. Marciniak A, Cohrs CM, Tsata V, Chouinard JA, Selck C, Stertmann J, et al. Using pancreas tissue slices for in situ studies of islet of Langerhans and acinar cell biology. Nat Protoc. 2014 Dec;9(12):2809–22.

106. Misra S, Moro CF, Del Chiaro M, Pouso S, Sebestyén A, Löhr M, et al. Ex vivo organotypic culture system of precision-cut slices of human pancreatic ductal adenocarcinoma. Sci Rep. 2019 Feb 14;9(1):2133.

107. Jiang X, Seo YD, Chang JH, Coveler A, Nigjeh EN, Pan S, et al. Long-lived pancreatic ductal adenocarcinoma slice cultures enable precise study of the immune microenvironment. Oncoimmunology. 2017;6(7):e1333210.

108. Seo YD, Jiang X, Sullivan KM, Jalikis FG, Smythe KS, Abbasi A, et al. Mobilization of CD8+ T Cells via CXCR4 Blockade Facilitates PD-1 Checkpoint Therapy in Human Pancreatic Cancer. Clin Cancer Res Off J Am Assoc Cancer Res. 2019 Jul 1;25(13):3934–45.

109. Naipal KAT, Verkaik NS, Sánchez H, van Deurzen CHM, den Bakker MA, Hoeijmakers JHJ, et al. Tumor slice culture system to assess drug response of primary breast cancer. BMC Cancer. 2016 Feb 9;16:78.

110. Pascual-García M, Bonfill-Teixidor E, Planas-Rigol E, Rubio-Perez C, Iurlaro R, Arias A, et al. LIF regulates CXCL9 in tumor-associated macrophages and prevents CD8+ T cell tumor-infiltration impairing anti-PD1 therapy. Nat Commun. 2019 11;10(1):2416.

111. Gerlach MM, Merz F, Wichmann G, Kubick C, Wittekind C, Lordick F, et al. Slice cultures from head and neck squamous cell carcinoma: a novel test system for drug susceptibility and mechanisms of resistance. Br J Cancer. 2014 Jan 21;110(2):479–88.

112. Majumder B, Baraneedharan U, Thiyagarajan S, Radhakrishnan P, Narasimhan H, Dhandapani M, et al. Predicting clinical response to anticancer drugs using an ex vivo platform that captures tumour heterogeneity. Nat Commun. 2015 Feb 27;6:6169.

113. Koerfer J, Kallendrusch S, Merz F, Wittekind C, Kubick C, Kassahun WT, et al. Organotypic slice cultures of human gastric and esophagogastric junction cancer. Cancer Med. 2016;5(7):1444–53.

114. Närhi K, Nagaraj AS, Parri E, Turkki R, van Duijn PW, Hemmes A, et al. Spatial aspects of oncogenic signalling determine the response to combination therapy in slice explants from Kras-driven lung tumours. J Pathol. 2018 May;245(1):101–13.

115. Nikolova T, Dvorak M, Jung F, Adam I, Krämer E, Gerhold-Ay A, et al. The γH2AX Assay for Genotoxic and Nongenotoxic Agents: Comparison of H2AX Phosphorylation with Cell Death Response. Toxicol Sci. 2014 Jul 1;140(1):103–17.

116. Duan WR, Garner DS, Williams SD, Funckes-Shippy CL, Spath IS, Blomme EAG. Comparison of immunohistochemistry for activated caspase-3 and cleaved cytokeratin 18 with the TUNEL method for quantification of apoptosis in histological sections of PC-3 subcutaneous xenografts. J Pathol. 2003 Feb;199(2):221–8.

117. Chun OK, Floegel A, Chung S-J, Chung CE, Song WO, Koo SI. Estimation of antioxidant intakes from diet and supplements in U.S. adults. J Nutr. 2010 Feb;140(2):317–24.

118. Institute of Medicine (US) Panel on Dietary Antioxidants and Related Compounds. Dietary Reference Intakes for Vitamin C, Vitamin E, Selenium, and Carotenoids [Internet]. Washington (DC): National Academies Press (US); 2000 [cited 2021 May 10]. Available from: http://www.ncbi.nlm.nih.gov/books/NBK225483/

119. Chen J. An original discovery: selenium deficiency and Keshan disease (an endemic heart disease). Asia Pac J Clin Nutr. 2012;21(3):320–6.

120. Hatfield DL, Berry MJ, Gladyshev VN. Selenium: Its Molecular Biology and Role in Human Health. Springer Science & Business Media; 2011. 596 p.

121. Jorgenson TC, Zhong W, Oberley TD. Redox imbalance and biochemical changes in cancer. Cancer Res. 2013 Oct 15;73(20):6118–23.

122. Glasauer A, Chandel NS. Targeting antioxidants for cancer therapy. Biochem Pharmacol. 2014 Nov 1;92(1):90–101.

123. Shih AY, Johnson DA, Wong G, Kraft AD, Jiang L, Erb H, et al. Coordinate Regulation of Glutathione Biosynthesis and Release by Nrf2-Expressing Glia Potently Protects Neurons from Oxidative Stress. J Neurosci. 2003 Apr 15;23(8):3394–406.

124. Balendiran GK, Dabur R, Fraser D. The role of glutathione in cancer. Cell Biochem Funct. 2004 Dec;22(6):343–52.

125. Foster SJ, Kraus RJ, Ganther HE. The metabolism of selenomethionine, Se-methylselenocysteine, their selenonium derivatives, and trimethylselenonium in the rat. Arch Biochem Biophys. 1986 Nov 15;251(1):77–86.

126. Nilsonne G, Sun X, Nyström C, Rundlöf A-K, Potamitou Fernandes A, Björnstedt M, et al. Selenite induces apoptosis in sarcomatoid malignant mesothelioma cells through oxidative stress. Free Radic Biol Med. 2006 Sep 15;41(6):874–85.

127. Husbeck B, Nonn L, Peehl DM, Knox SJ. Tumor-selective killing by selenite in patient-matched pairs of normal and malignant prostate cells. The Prostate. 2006 Feb 1;66(2):218–25.

128. Olm E, Fernandes AP, Hebert C, Rundlöf A-K, Larsen EH, Danielsson O, et al. Extracellular thiol-assisted selenium uptake dependent on the x(c)- cystine transporter explains the cancer-specific cytotoxicity of selenite. Proc Natl Acad Sci U S A. 2009 Jul 7;106(27):11400–5.

129. Cooper AJL, Pinto JT, Krasnikov BF, Niatsetskaya ZV, Han Q, Li J, et al. Substrate specificity of human glutamine transaminase K as an aminotransferase and as a cysteine S-conjugate beta-lyase. Arch Biochem Biophys. 2008 Jun 1;474(1):72–81.

130. Zeng H, Wu M, Botnen JH. Methylselenol, a selenium metabolite, induces cell cycle arrest in G1 phase and apoptosis via the extracellular-regulated kinase 1/2 pathway and other cancer signaling genes. J Nutr. 2009 Sep;139(9):1613–8.

131. Zeng H, Briske-Anderson M, Wu M, Moyer MP. Methylselenol, a selenium metabolite, plays common and different roles in cancerous colon HCT116 cell and noncancerous NCM460 colon cell proliferation. Nutr Cancer. 2012;64(1):128–35.

132. Nian H, Bisson WH, Dashwood W-M, Pinto JT, Dashwood RH. Alpha-keto acid metabolites of organoselenium compounds inhibit histone deacetylase activity in human colon cancer cells. Carcinogenesis. 2009 Aug;30(8):1416–23.

133. Lee HS, Park SB, Kim SA, Kwon SK, Cha H, Lee DY, et al. A novel HDAC inhibitor, CG200745, inhibits pancreatic cancer cell growth and overcomes gemcitabine resistance. Sci Rep. 2017 Jan 30;7:41615.

134. Jiao F, Hu H, Yuan C, Jin Z, Guo Z, Wang L, et al. Histone deacetylase 3 promotes pancreatic cancer cell proliferation, invasion and increases drug-resistance through histone modification of P27, P53 and Bax. Int J Oncol. 2014 Oct;45(4):1523–30.

135. Selvam AK, Björnstedt M. A Novel Assay Method to Determine the β-Elimination of Se-Methylselenocysteine to Monomethylselenol by Kynurenine Aminotransferase 1. Antioxidants. 2020 Feb;9(2):139.

136. Brodin O, Eksborg S, Wallenberg M, Asker-Hagelberg C, Larsen EH, Mohlkert D, et al. Pharmacokinetics and Toxicity of Sodium Selenite in the Treatment of Patients with Carcinoma in a Phase I Clinical Trial: The SECAR Study. Nutrients. 2015 Jun 19;7(6):4978–94.

137. Bosman F, Carneiro F, Hruban R, Theise N, editors. WHO Classification of Tumours of the Digestive System. 4th ed. Lyon: International Agency for Research on Cancer; 2010.

138. Greijer AE, van der Wall E. The role of hypoxia inducible factor 1 (HIF-1) in hypoxia induced apoptosis. J Clin Pathol. 2004 Oct;57(10):1009–14.

139. Radreau P, Rhodes JD, Mithen RF, Kroon PA, Sanderson J. Hypoxia-inducible factor-1 (HIF-1) pathway activation by quercetin in human lens epithelial cells. Exp Eye Res. 2009 Dec;89(6):995–1002.

140. van Uden P, Kenneth NS, Rocha S. Regulation of hypoxia-inducible factor-1α by NF-κB. Biochem J. 2008 Jun 15;412(Pt 3):477–84.

141. Fujioka S, Niu J, Schmidt C, Sclabas GM, Peng B, Uwagawa T, et al. NF-κB and AP-1 Connection: Mechanism of NF-κB-Dependent Regulation of AP-1 Activity. Mol Cell Biol. 2004 Sep;24(17):7806–19.

142. Evans DB, Rich TA, Byrd DR, Cleary KR, Connelly JH, Levin B, et al. Preoperative chemoradiation and pancreaticoduodenectomy for adenocarcinoma of the pancreas. Arch Surg Chic Ill 1960. 1992 Nov;127(11):1335–9.

143. Ku H-C, Cheng C-F. Master Regulator Activating Transcription Factor 3 (ATF3) in Metabolic Homeostasis and Cancer. Front Endocrinol. 2020;11:556.

144. Xu H, Shen Z, Xiao J, Yang Y, Huang W, Zhou Z, et al. Acetylcholinesterase overexpression mediated by oncolytic adenovirus exhibited potent anti-tumor effect. BMC Cancer. 2014 Sep 15;14:668.

145. Koga A, Sato N, Kohi S, Yabuki K, Cheng X-B, Hisaoka M, et al. KIAA1199/CEMIP/HYBID overexpression predicts poor prognosis in pancreatic ductal adenocarcinoma. Pancreatol Off J Int Assoc Pancreatol IAP Al. 2017 Feb;17(1):115–22.

146. Qi Y, Xu R. Roles of PLODs in Collagen Synthesis and Cancer Progression. Front Cell Dev Biol. 2018;6:66.

147. Wasinski B, Sohail A, Bonfil RD, Kim S, Saliganan A, Polin L, et al. Discoidin Domain Receptors, DDR1b and DDR2, Promote Tumour Growth within Collagen but DDR1b Suppresses Experimental Lung Metastasis in HT1080 Xenografts. Sci Rep. 2020 Feb 11;10(1):2309.

148. Cao XP, Cao Y, Li WJ, Zhang HH, Zhu ZM. P4HA1/HIF1α feedback loop drives the glycolytic and malignant phenotypes of pancreatic cancer. Biochem Biophys Res Commun. 2019 Aug 27;516(3):606–12.

149. Malgerud L, Lindberg J, Wirta V, Gustafsson-Liljefors M, Karimi M, Moro CF, et al. Bioinformatory-assisted analysis of next-generation sequencing data for precision medicine in pancreatic cancer. Mol Oncol. 2017 Oct;11(10):1413–29.